Annual Reviews in Control 62 (2026) 101083

Contents lists available at ScienceDirect

Annual Reviews in Control

journal homepage: www.elsevier.com/locate/arcontrol

Review Article

Dynamic event-triggered control of PDE systems via backstepping: *Application to open-canal flow stabilization*☆

Mamadou Diagne [a,*], Eranda Somathilake [a], Bhathiya Rathnayake [b]

[a] Department of Mechanical and Aerospace Engineering, University of California San Diego, La Jolla, CA, 92093, USA
[b] The Ralph O'Connor Sustainable Energy Institute (ROSEI), Johns Hopkins University, Baltimore, MD, 21211, USA

ARTICLE INFO

Keywords:
Backstepping control design
Coupled hyperbolic systems
Event-triggered control
Periodic event-triggered control
Self-triggered control
Water systems

ABSTRACT

Modern control systems, composed of interconnected plants, actuators, and sensors, can be stabilized efficiently through event-triggered control (ETC), which reduces sensing, communication, and actuation costs while guaranteeing satisfactory closed-loop performance. This review article presents *dynamic* event-triggered boundary control strategies for partial differential equations (PDEs), developed via PDE backstepping, with an application to the linearized hyperbolic Saint-Venant model described by 2×2 coupled hyperbolic PDEs in a canonical form. Three classes of event-triggering mechanisms (ETMs) are discussed: regular ETC (R-ETC), performance-barrier ETC (P-ETC), and switching ETC (S-ETC). Stability is established in the spatial L^2 norm using Lyapunov-based analysis, and Zeno phenomena are ruled out by either establishing the existence of or enforcing explicit minimal dwell-times (MDTs). All designs exploit auxiliary dynamic variables that govern the ETMs, and can be generalized through performance-barrier functions to extend the average dwell-times. R-ETC guarantees L^2 global exponential convergence (GEC), whereas S-ETC achieves global exponential stability (GES) by leveraging carefully constructed *switching* dynamic variables. To eliminate continuous monitoring of the triggering condition, R-ETC, P-ETC, and S-ETC are further refined into periodic ETC (PETC), requiring only periodic evaluation of the ETMs, and self-triggered control (STC), which computes the next update time at the current event without monitoring any triggering condition. The viability of our frameworks is demonstrated for an open-canal flow regulation using downstream gate actuation. In this setting, reducing the number of updates of the actuation signal prolongs actuator life cycle. Extensive numerical simulations confirm the effectiveness of all ETC strategies presented. The modular nature of these designs makes them applicable to other classes of PDE or PDE-ODE cascade systems.

Contents

1. Introduction 2
   1.1. The concept and a brief history of event-triggered control design 2
   1.2. Event-triggered control of PDEs 3
   1.3. Periodic event-triggered and self-triggered control of PDEs 3
   1.4. Performance barrier event-triggered control (P-ETC) 3
   1.5. Gain scheduling and adaptive event-triggered control 4
   1.6. Motivation for the event-based control of open-canals 4
   1.7. Contributions 4
   1.8. Notations 5
2. Principles of event-triggered control 5
   2.1. From sampled-data to event-triggered control 5
   2.2. Static and dynamic ETMs for PDE systems 5
3. Emulation of the continuous-time boundary control law of the Saint-Venant model 6
   3.1. Governing equations of the Saint-Venant model 6
   3.2. Continuous-time controller design 8

☆ This work was funded by the National Science Foundation (NSF) CAREER Award CMMI-2302030 and the NSF grant CMMI-2222250.
* Corresponding author.
E-mail address: mdiagne@ucsd.edu (M. Diagne).

https://doi.org/10.1016/j.arcontrol.2026.101083
Received 19 January 2026; Received in revised form 31 August 2026; Accepted 31 October 2026
1367-5788/© 2026 Published by Elsevier Ltd.

3.3. Emulation of the PDE backstepping control ... 8
4. Regular event-triggered control ... 9
4.1. Continuous-time event-triggered control ... 9
4.2. Periodic event-triggered control ... 10
4.3. Self-triggered control ... 11
5. Performance-barrier event-triggered control ... 12
5.1. Performance-barrier continuous-time event-triggered control ... 13
5.2. Performance-barrier periodic event-triggered control ... 14
5.3. Performance-barrier self-triggered control ... 14
6. Dynamic switching event-triggered control ... 15
6.1. Switching continuous-time event-triggered control ... 15
6.2. Switching periodic event-triggered control ... 16
6.3. Switching self-triggered control ... 17
7. Numerical simulations ... 17
8. Concluding remarks and perspectives ... 18
Declaration of competing interest ... 20
Data availability ... 20
References ... 20

1. Introduction

1.1. The concept and a brief history of event-triggered control design

Event-triggered control (ETC) is a feedback strategy that accounts for both the system dynamics and the communication between sensors and actuators. As a resource-aware control design, its goal is to save sensing, actuation, and communication (e.g. bandwidth for signal transmission) resources during the execution of control tasks while maintaining proper closed-loop stability and performance. Unlike conventional sampled-data control, ETC updates the control signal only when certain conditions are met. This makes ETC more appealing than aperiodic sampled-data control that relies on open-loop updates and often leads to a conservative maximum allowable sampling interval. Fundamentally, ETC consists of two primary elements: a *feedback control law* that ensures the closed-loop system's stability, and an *event-triggering mechanism (ETM)* that determines when the control input should be computed and transmitted to the actuator. In the literature, two main approaches are commonly used to design the feedback control law: *emulation* and *co-design*. The *emulation* approach applies a pre-designed continuous-time feedback law to the plant through a zero-order hold (ZOH) between successive event times. By contrast, the *co-design* approach consists of a concurrent construction of the two components of ETC to achieve the desired stability properties. ETMs are classified in two main categories: *static* and *dynamic*. Static ETMs are based on fixed rules and often require access to the full system state, whereas dynamic ETMs use auxiliary dynamic variables, which can lead to less frequent event triggers and offer greater flexibility such as being compatible with observer-based implementations.

Sampled-data Control. From a historical perspective, the development of sampled-data control has evolved through several stages and reflects contributions from many researchers. Foundational developments in sampling theory can be traced to Nyquist and Shannon, whose work established fundamental principles underlying the sampling and reconstruction of continuous-time signals (Nyquist, 1928; Shannon, 1949). These developments were subsequently connected more directly to feedback control through the early contributions (Linvill, 1951; Ragazzini & Zadeh, 1952). These contributions were followed by advances introducing a unified framework for the analysis of sampling and sampled-data systems, including a state-space perspective and stability analysis in Kalman and Bertram (1959) (see the relatively recent survey (Yamamoto, 2019) and references therein). With the emergence of digital and computer-based control, further results enabled the analysis, design, and implementation of computer-controlled systems through sampled-data design (Åström & Wittenmark, 1984). The subsequent progress of modern sampled-data control occurred with the conception of optimal H_2 and H_∞ sampled-data control in Chen and Francis (1995). Parallel developments established foundations for nonlinear sampled-data control and digital implementation (Nešić & Laila, 2002; Nešić & Teel, 2004; Nešić et al., 1999; Nešić, Teel & Sontag, 1999). Thus, rather than being attributable to a single precursor, modern sampled-data control is the outcome of a cumulative development spanning sampling theory, early sampled-data feedback systems, state-space methods, digital control, and nonlinear systems. In a broad sense, the advent of digital computers has prompted the emergence of periodic and aperiodic sampled-data control systems since the mid-20th century (Albertos & Salt, 2011; Athans, 1972; Dorf et al., 1962; Gupta, 1963; Jury, 1956; Meier et al., 1967; Tomovic & Bekey, 1966; Widrow, 1960; Zhang et al., 2023). These developments for finite-dimensional systems naturally motivated the extension of sampled-data control to distributed-parameter systems, where the underlying dynamics are governed by partial differential equations (PDEs) and the interplay between temporal sampling and spatially distributed dynamics introduces additional analytical challenges. Notable contributions in this direction include the works of Fridman and co-authors (Fridman & Bar Am, 2013; Kang & Fridman, 2022; Selivanov & Fridman, 2017; Wang & Fridman, 2024) as well as that of Karafyllis, Krstić and co-authors (Ahmed-Ali et al., 2017; Karafyllis & Krstić, 2012, 2016, 2017, 2018; Koga et al., 2021). Related developments for parabolic and hyperbolic PDEs can be found in Cheng et al. (2009), Rathnayake and Diagne (2025), Rathnayake, Diagne, and Karafyllis (2022). The progress on sampled-data control provided a foundation for the subsequent development of event-based control strategies for ordinary differential equation (ODE) and PDE systems.

Event-triggered Control. Building on this foundation, the event-based PID control approach proposed in Årzén (1999) and the event-driven sampling method for first-order stochastic systems in Åström and Bernhardsson (1999), are among the seminal contributions that shaped subsequent developments in the field. Thereafter, following Tabuada (2007), ETC has advanced rapidly, with significant developments in theory, design methodologies, and practical implementations for systems that are governed by ODEs. Fascinating ETC results have been reported on linear and nonlinear ODE systems that are deterministic (Abdelrahim et al., 2016; Ghodrat & Marquez, 2023; Girard, 2015; Marchand et al., 2013; Postoyan et al., 2015; Tallapragada & Chopra, 2013) (with output feedback designs found in Donkers and Heemels (2012), Zhang et al. (2021b) and time-delay systems covered in Nozari et al. (2020), Zhang et al. (2021a)) or stochastic (Demirel et al., 2019; Gao et al., 2018; Luo & Deng, 2020; Wang et al., 2023, 2017; Zhang & Fridman, 2021). The references cited above are representative, rather than exhaustive, of the extensive developments in ETC for finite-dimensional systems. A detailed review of ETC for ODE systems can be found in recent review articles, such as Hertneck et al. (2026), as well

as in Hashimoto et al. (2021), which focuses on population models of epidemic spreading. Our focus is instead directed towards the event-based control of PDE systems, which poses a distinct set of challenges compared to those encountered in ODEs.

1.2. Event-triggered control of PDEs

Recently, ETC for PDEs has gained increasing attention, motivated in part by the growing prevalence of networked control systems (NCSs) (Bemporad et al., 2010; Hespanha et al., 2007). ETC schemes for PDE systems based on static event-triggers have been used in works such as Espitia et al. (2016, 2021), Koudohode et al. (2022), Rathnayake and Diagne (2022), Selivanov and Fridman (2016), while dynamic event-triggers have been explored in Espitia (2020), Kang et al. (2023), Lhachemi (2024), Rathnayake, Diagne, Espitia and Karafyllis (2022), Wang and Krstić (2023a) and the references therein. It is worth noting that under static schemes only a few exceptions allow output feedback designs (Espitia et al., 2016; Selivanov & Fridman, 2016).

ETC for parabolic PDEs has been studied in works such as Espitia et al. (2021), Kang et al. (2023), Katz et al. (2021), Koudohode et al. (2024), Lhachemi (2024), Rathnayake and Diagne (2022), Rathnayake, Diagne, Espitia and Karafyllis (2022), Rathnayake, Diagne, and Karafyllis (2022), Wang and Krstić (2023a). Full-state feedback can be achieved under static triggering mechanisms for reaction–diffusion (RD) PDEs using the backstepping approach (Espitia et al., 2021; Koudohode et al., 2024; Rathnayake & Diagne, 2022). Dynamic triggering mechanisms are presented in Rathnayake, Diagne, Espitia and Karafyllis (2022), Rathnayake, Diagne, and Karafyllis (2022), Wang and Krstić (2023a), with Wang and Krstić (2023a) developing a full-state adaptive ETC control design, and Rathnayake, Diagne, Espitia and Karafyllis (2022), Rathnayake, Diagne, and Karafyllis (2022) introducing both sampled-data and ETC output-feedback designs. Notably, within the context of PDE backstepping design, (Rathnayake, Diagne, Espitia & Karafyllis, 2022; Rathnayake, Diagne, & Karafyllis, 2022) identified a class of RD PDEs with Robin boundary condition for which dynamic ETC can be applied in both full-state and output-feedback configurations. Observer-based modal decomposition methods for dynamic ETC of RD PDEs are developed in Katz et al. (2021), Lhachemi (2024). The authors of Kang et al. (2023) introduce a full-state-feedback dynamic ETC method for nonlinear RD PDEs with in-domain (distributed) actuation. Results on **ETC for hyperbolic PDEs** can be found in Baudouin et al. (2019), Diagne and Karafyllis (2021), Espitia (2020), Espitia et al. (2016), Koudohode et al. (2022), Strecker et al. (2024), Sun et al. (2025), Wang and Krstić (2021, 2022b, 2022c, 2023b), Wang et al. (2021) in both output and full-state feedback settings. Static triggering schemes have been applied to linear hyperbolic systems (Espitia et al., 2016), damped wave equations (Baudouin et al., 2019; Koudohode et al., 2022), 2×2 semilinear hyperbolic systems (Strecker et al., 2024), and scalar nonlinear PDEs of highly re-entrant manufacturing processes (Diagne & Karafyllis, 2021) (relevant to the chips and semiconductors industry). Dynamic triggering for the boundary control of 2×2 linear hyperbolic PDEs leveraging PDE backstepping is developed in Espitia (2020), Wang and Krstić (2021, 2022b, 2022c, 2023b), Wang et al. (2021) and references therein.

1.3. Periodic event-triggered and self-triggered control of PDEs

Despite their theoretical appeal, ETC schemes for ODE and PDE systems typically rely on continuous monitoring of triggering conditions, a requirement that limits their suitability for digital implementation. In the present review article, these strategies are referred to as *continuous-time event-triggered control (CETC)*. To relax the continuous monitoring of the system and the actuator state, *periodic event-triggered control (PETC)* has been proposed (Heemels et al., 2013), where the triggering condition is evaluated periodically whereas the control input is updated only when necessary in an aperiodic manner. Another alternative is *self-triggered control (STC)* (Heemels et al., 2012), where the next update time is predicted using the data available at the current event. By allowing the triggering condition or the next event time to be computed within sampled-data digital frameworks, PETC and STC provide practical mechanisms to bridge the gap between ETC theory and digital implementation. However, CETC and PETC can provide greater opportunities to react to unforeseen disturbances or measurement variations between triggering instants, since the triggering condition is monitored continuously or periodically, respectively. In contrast, STC determines the next triggering instant based on information available at the current triggering instant and therefore does not directly account for changes occurring between triggering instants. Nevertheless, STC schemes can also be designed to explicitly account for disturbances and measurement noise (Brunner et al., 2019; Gleizer & Mazo, 2020). Recent years have witnessed significant advances in PETC (Borgers et al., 2018; Fu & Mazo, 2018; Heemels & Donkers, 2013; Heemels et al., 2013; Linsenmayer et al., 2019; Seidel et al., 2024; Wang et al., 2020) and STC (Anta & Tabuada, 2010; Cao et al., 2023; Heemels et al., 2012; Mazo et al., 2009; Mazo & Tabuada, 2008; Wan et al., 2021; Yang et al., 2019; Yi et al., 2019) for ODE systems. In contrast, extensions of event-triggered strategies to PDE systems remain limited, with existing works on ETC including Rathnayake and Diagne (2024b), Selivanov and Fridman (2016), Somathilake et al. (2025), Wakaiki and Sano (2020, 2022). Selivanov and Fridman (2016) introduces a PETC scheme for networks of semi-linear diffusion PDEs with *in-domain* actuation and either distributed or point measurements. Building on semigroup theory, Wakaiki and Sano (2020) develops a full-state feedback PETC framework for infinite-dimensional systems with unbounded control operators, whereas Wakaiki and Sano (2022) proposes a full-state feedback STC design for systems with bounded control operators. More recently, using the PDE backstepping control framework (Rathnayake & Diagne, 2024b) presents the first PETC and STC backstepping boundary control design for a class of RD PDEs using only boundary measurements. The approach has been extended to 2×2 hyperbolic PDEs in Somathilake et al. (2025).

1.4. Performance barrier event-triggered control (P-ETC)

The terminology P-ETC (not to be confused with PETC) uses the words "performance" and "barrier" in a way that is distinct from their usage in the safety-critical control literature (Ames et al., 2019, 2017; Krstić, 2024; Taylor et al., 2021), where they relate to safety guarantees. In our setting, performance refers to the nominal decay of the Lyapunov function, serving as a measure of system convergence, while barrier denotes a boundary or threshold that the system should avoid crossing. Together, the *performance-barrier* terminology encapsulates the idea of comparing the Lyapunov function's behavior to an acceptable nominal decrease, treating it as a boundary that should not be violated. Regular dynamic ETMs force a monotonic decrease in the Lyapunov function of the closed-loop system by ensuring its time derivative remains strictly negative. In terms of performance, this guarantees the Lyapunov function decreases faster than a specific exponentially decaying signal, which incorporates the initial data. We refer to this latter signal as the *performance-barrier*. Allowing some flexibility in the Lyapunov function's behavior — letting it deviate from a strict monotonic decrease but still respecting the performance-barrier — one can achieve longer dwell-times between events leading to less frequent control updates.

This idea was carried out in Ong and Cortés (2024) for ODEs, which develops an ETC design that integrates both the time derivative and the value of the Lyapunov function into the ETM. The idea underlying P-ETC, namely, bounding the Lyapunov function with a decreasing reference function rather than enforcing pointwise monotonic decrease, predates the terminology of Ong and Cortés (2024). Comparing the Lyapunov decay against a decreasing reference function was pioneered

in Wang and Lemmon (2008), though without a guarantee tied to a prescribed convergence rate. This was extended to a prescribed Lyapunov-based performance guarantee in Mazo et al. (2010) and Szymanek et al. (2019) in a self-triggered setting and a PETC setting respectively. Additionally, prior to Ong and Cortés (2024), the question of optimal sampling has been tackled in Bahavarnia et al. (2017), where computing the controller and the sampling schedule of linear time-invariant (LTI) systems via self-triggered sparse optimal control (SSOC) laws is defined as a sparse optimization problem. The optimal control law of Bahavarnia et al. (2017), Etienne et al. (2022) globally stabilizes the LTI system, maximizes the inter-execution time and provides guaranteed closed-loop performance bounds. Furthermore, optimal sampling (Bini & Buttazzo, 2014; Tripathy et al., 2017), optimal event transmission scheduling (Leong et al., 2017), and *act-and-wait* control that preserve resources by reducing "ON" time of the actuator can be found in Imer and Basar (2005, 2006). However, act-and-wait control (Imer & Basar, 2005, 2006) should be interpreted as an *event-triggered sparse control* rather than *sparse event-triggered control* as achieved with the performance barrier design in Ong and Cortés (2024) and its extension to parabolic and hyperbolic PDE systems in Rathnayake et al. (2024, 2025), Zhang et al. (2025).

1.5. Gain scheduling and adaptive event-triggered control

Event-triggered gain scheduling control. In a broader sense, ETC in its various schemes is useful to gain scheduling control design. ETC and STC gain scheduled control of linear systems with input constraints is proposed in Zhang et al. (2022) while Coutinho and Palhares (2022) presents a co-design dynamic event-triggered gain-scheduling control for a class of nonlinear systems equivalent to a local polytopic model. Further results include Coutinho et al. (2022), which achieves gain-scheduling for discrete-time nonlinear systems described by quasi-LPV systems (see also Pessim et al. (2025) for an application to consensus of LPV multi-agent systems). The field of event-triggered gain scheduling control of PDE systems is less explored with only a few results including the boundary control of a scalar RD PDE with space- and time-dependent reaction coefficient (Karafyllis et al., 2021) and that of a 2×2 hyperbolic PDE with space- and time-dependent coupling coefficients (Espitia & Auriol, 2025). Espitia and Auriol (2025), Karafyllis et al. (2021) establish global exponential stability (GES) using either a static triggering mechanism in conjunction with a small-gain approach or a Lyapunov-based analysis. Nonetheless, the co-design of event-triggered gain-scheduling control for PDE systems remains unexplored, as do periodic and self-triggered gain scheduling control.

Event-triggers in adaptive control. Since the late 1980s, sampled-data and related event-based mechanisms have been employed in adaptive control, notably in Miller and Davison (1988, 1991) and Hespanha et al. (2003), Morse (1996) (see the prologue of Karafyllis and Krstić (2025) for further details). In recent years, the concept of ETC has led to recent developments in adaptive control through *batch least-squares identifiers-based adaptive control (BaLSI)* applied to both ODE and PDE systems. BaLSI guarantees finite-time identification of the system's unknown constant parameters and exponential regulation of uncertain nonlinear ODEs (Karafyllis et al., 2020), with applications such as two-link robot control (Bagheri et al., 2021). As well, BaLSI-based adaptive control has been applied to RD PDEs (Wang & Krstić, 2023a), hyperbolic systems (Wang & Krstić, 2021, 2023b; Wang et al., 2021), and delay-adaptive control of hyperbolic PDE-ODE systems (Wang & Diagne, 2024), expanding existing adaptive backstepping approaches for PDEs (Krstić & Smyshlyaev, 2008).

1.6. Motivation for the event-based control of open-canals

Automation of open-channel flow can lead to significant savings in water, particularly in irrigation canals (Conde et al., 2021; Eliades et al., 2023; Simonovic & Akter, 2006; Wahlin & Zimbelman, 2018). However, continuous-time centralized control of large-scale open-channel networks can impose substantial communication and computational burdens, particularly when sensors and actuators are distributed over large distances, resulting in significant network traffic and communication costs (Ge et al., 2021). Power management is also a major concern for remote sensors and actuators deployed along water channels, as such equipment may have limited power availability (Ge et al., 2021). These considerations have spurred increasing interest in control strategies that reduce communication and computational requirements while maintaining satisfactory control performance (Dolk & Heemels, 2017; Ge et al., 2021).

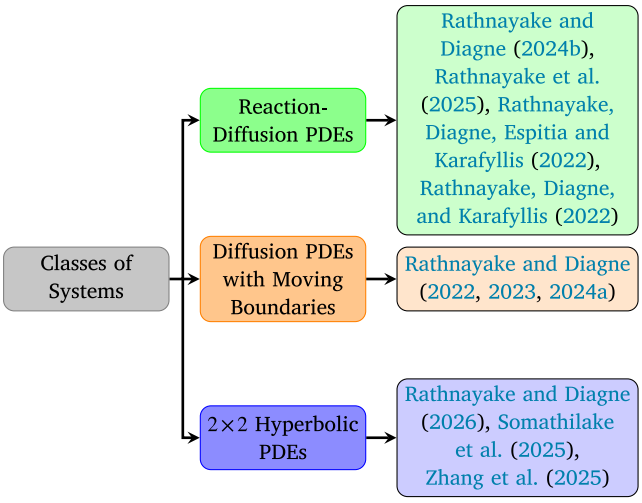

Fig. 1. Classes of systems that our dynamic CETC, PETC and STC can stabilize with GEC or GES.

These challenges motivate the adoption of ETC, which activates control updates sparsely thereby reducing the use of network bandwidth and energy. From a PDE-control standpoint, *Saint-Venant* equations model the spatial distribution of water height and velocity over time for open-channel flow (Barré de Saint-Venant, 1871). The model has been used to regulate open-channel flow in numerous contributions. Continuous-time control (CTC) strategies include frequency domain based control (Litrico & Fromion, 2009), linear quadratic regulator based control methods (Balogun et al., 1988), model predictive control (Nasir et al., 2021), and Lyapunov based control methods (Coron et al., 1999). Results on models of Saint-Venant integrating sediment dynamics can be found in Diagne et al. (2012), Ababacar Diagne et al. (2017), Mamadou Diagne et al. (2017), Prieur and Mazenc (2012), Prieur and Winkin (2018), Somathilake and Diagne (2024). Backstepping boundary control for a system of 2×2 linear hyperbolic PDEs given in Vazquez et al. (2011) can be applied to control of the linearized Saint-Venant equations.

1.7. Contributions

This review article presents recently developed dynamic ETC strategies for 1-D 2×2 linear coupled hyperbolic PDEs with application to open canal flow. The possibility of Zeno behavior is excluded by either proving the existence of or enforcing a uniform positive minimal dwell-time (MDT) between consecutive events. Furthermore, the well-posedness of the closed-loop system and the global exponential convergence (GEC) or GES of the solutions under the ETC schemes of concern are established. The event-triggers that are presented in this article are versatile and applicable to various classes of PDEs as illustrated by Fig. 1. Two classes of dynamic triggering mechanisms are employed to design CETC, PETC, STC and P-ETC (Rathnayake & Diagne, 2024a, 2026; Rathnayake et al., 2025; Somathilake et al., 2025; Zhang et al., 2025).

For the **dynamic triggering approach with GEC guarantees,** the PETC framework is obtained through a redesign of the CETC triggering functions (Somathilake et al., 2025) to permit periodic evaluation. The PETC mechanism is inherently Zeno-free and retains the well-posedness and closed-loop properties of CETC with the state variables decaying to zero in the spatial L^2 norm at the same rate. The STC design uses a uniformly and positively lower-bounded function of the state to determine the waiting time until the next event. This ensures Zeno-free operation and preserves both the well-posedness and the stability of the closed-loop system. Moreover, the STC maintains the global exponential convergence of CETC, with signals decaying to zero in the spatial L^2 norm.

For the **dynamic switching (S) triggering approach with GES guarantees** (Rathnayake & Diagne, 2026), S-CETC design enforces a MDT, $\tau > 0$, preventing Zeno behavior. Unlike prior works (Demir et al., 2024b; Espitia et al., 2022a, 2022b, 2020; Rathnayake & Diagne, 2024a; Rathnayake et al., 2024; Rathnayake, Diagne, Espitia & Karafyllis, 2022; Rathnayake, Diagne, & Karafyllis, 2022; Wang & Krstić, 2021, 2022b, 2023a; Wang et al., 2021; Zhang et al., 2025), which require proof of a MDT, this method uses a switching variable that remains strictly non-zero between t_j and $t_j + \tau$, decreasing afterward until its zero-crossing triggers the next event. While time-regularization and switching variables can be found in Kang et al. (2023), Katz et al. (2021), the approach in Rathnayake and Diagne (2026) draws from the method proposed in Dolk et al. (2014) for ODE networked systems. The proof of GES requires the construction of a Lyapunov function combining the plant's infinite-dimensional state, the switching variable, and a state-independent dynamic reset modulated by sampling error. The S-PETC design defines a triggering condition that is evaluated periodically rather than continuously, with the sampling period upper-bounded by the MDT derived under S-CETC (Rathnayake & Diagne, 2026). This ensures the triggering mechanism preserves GES while inherently avoiding Zeno behavior. In contrast, S-STC approach does not require monitoring a triggering condition. GES under S-STC is established via Lyapunov analysis, and unlike S-CETC, S-PETC, or prior static (Espitia et al., 2021; Koga et al., 2023; Koudohode et al., 2024; Rathnayake & Diagne, 2022; Strecker et al., 2024) or dynamic (Demir et al., 2024a, 2024b; Espitia, 2020; Espitia et al., 2022a, 2022b, 2020; Rathnayake & Diagne, 2023, 2024a; Rathnayake et al., 2024; Rathnayake, Diagne, Espitia & Karafyllis, 2022; Rathnayake, Diagne, & Karafyllis, 2022; Somathilake et al., 2025; Wang & Krstić, 2021, 2022b, 2022c, 2023a; Wang et al., 2021; Zhang et al., 2025) ETC schemes, S-STC relies solely on measurements at the current and previous event times to schedule the next triggering instant. A summary of the event-triggered mechanisms reviewed in the article are depicted in Fig. 2.

The paper is organized as follows. Section 2, succinctly restates ETC design techniques employed in this article. Section 3 introduces the Saint-Venant open channel fluid flow model, its CTC design and emulation. Section 4 introduces CETC, PETC, and STC designs based on a dynamic ETM. Section 5 presents the P-ETC designs for CETC, PETC, and STC. Section 6 introduces CETC, PETC, and STC designs based on a dynamic switching ETM. Numerical simulations illustrating the triggering mechanisms are presented in Section 7. Concluding remarks and possible future directions are discussed in Section 8.

1.8. Notations

Let $\mathbb{R}$ be the set of real numbers, $\mathbb{R}_{>0}$ be the set of positive real numbers, and $\mathbb{R}_{\geq 0}$ be the set of nonnegative real numbers including zero. Define the constant $\ell \in \mathbb{R}_{>0}$. Let $\mathbb{N}$ be the set of natural numbers including 0, and let $\mathbb{N}_{>0}$ be the set of natural numbers greater than 0. By $L^2(0,\ell)$, we denote the equivalence class of Lebesgue measurable functions $f : [0,\ell] \to \mathbb{R}$ such that $\|f\|_{L^2((0,\ell);\mathbb{R})} = (\int_0^\ell |f(x)|^2 dx)^{1/2} < \infty$. Let $u : [0,\ell]\times\mathbb{R}_{\geq 0} \to \mathbb{R}$ be given. $u[t]$ denotes the profile of u at a certain $t \geq 0$, *i.e.*, $(u[t])(x) = u(x,t)$, for all $x \in [0,\ell]$. Define $C^0(I; L^2((0,\ell);\mathbb{R}))$ as the space of continuous functions $u[t]$ for an interval $I \subseteq \mathbb{R}_{\geq 0}$ such that $I \ni t \to u[t] \in L^2((0,\ell);\mathbb{R})$.

2. Principles of event-triggered control

2.1. From sampled-data to event-triggered control

Sampled-data control and time regularization.

Sampled-data control stands as the most straightforward way to bridge the gap between CTC and digital controllers. As illustrated in Fig. 3, a sampled-data control input is updated according to a predetermined sampling schedule denoted $I = \{t_k\}_{k\in\mathbb{N}}, t_0 = 0$, where $t_{k+1} - t_k \leq \tau_{mud}$, $\forall k \in \mathbb{N}$ $t_k \to \infty$ as $k \to \infty$. The maximum upper diameter, namely, the maximum sampling interval, τ_{mud}, typically derived from Lyapunov-based small-gain arguments or linear matrix inequality (LMI) criteria, must be selected conservatively to guarantee stability and performance. In the worst case, sufficiently frequent control updates are essential to prevent the closed-loop system from diverging or evolving along unstable trajectories during the open-loop operation separating consecutive sampling times. We refer the reader to Section 1.1 for a detailed discussion of sampled-data control of both ODE and PDE systems.

Event-triggered control.

Alternatively, ETC introduces feedback into the control update tasks as shown in Fig. 4. The control input is updated only when a certain condition related to the system states is satisfied, and such an occurrence is referred to as an *event*. This feedback integration means the schedule of control update times is no longer restricted by a worst-case scenario and must satisfy $t_j \to \infty$ as $j \to \infty$, leading to significantly sparser updates than traditional sampled-data control.

2.2. Static and dynamic ETMs for PDE systems

Consider a one-dimensional scalar PDE with spatially distributed state $u(x,t)$, $x \in (0,\ell)$, and boundary actuation at $u(\ell,t)$.

A typical **static triggering mechanism** specifies a condition under which the control signal $U(t_k)$, $k \in \mathbb{N}$, is updated at the next triggering instant t_{k+1} (e.g. Tabuada (2007) for ODE systems and Rathnayake and Diagne (2022) for cascade PDE-ODE systems). This condition is determined based on the deviation from the emulated continuous-time input $U(t)$, referred to as the *input holding error,* $d(t)$, together with a measure of the distributed state $u[t]$. As formulated below, the input deviation is directly compared with a state-dependent function f_s defined in terms of the plant's state norm at the last triggering instant $\|u[t_k]\|$ and at the current-time $\|u[t]\|$.

$$t_{k+1} = \inf\left\{t > t_k \middle| d^2(t) > f_s\left(u[t_k], u[t]\right)\right\},$$

with $t_0 = 0$, where

$$d(t) := U(t_k) - U(t), \text{ for } t \in [t_k, t_{k+1}), k \in \mathbb{N}.$$

The triggering ensures

$$d^2(t) \leq f_s\left(u[t_k], u[t]\right), \forall t \in \left[0, \sup\{t_k\}_{k\in\mathbb{N}}\right).$$

A **dynamic triggering mechanism,** as opposed to its static counterparts, involves an auxiliary variable whose time evolution depends on the *input holding error,* $d(t)$, as well as the norm of the PDE state, $\|u[t]\|$. The additional *dynamic* variable, $m(t)$, sparses the event-triggers. Such dynamic variables have been extensively employed in the context of ODEs, with seminal contributions found in Girard (2015), Seuret and Prieur (2011). Compared to static ETMs (Mazo et al., 2010; Wang & Lemmon, 2008), the auxiliary variable can be viewed as a filter applied to a static triggering condition, effectively filtering both the input holding error and a measure of the plant state (Dolk et al., 2014; Girard, 2015). A classical dynamic ETM is given below with the next triggering instant defined as

$$t_{k+1} = \inf\left\{t > t_k \middle| d^2(t) > m(t)\right\},$$

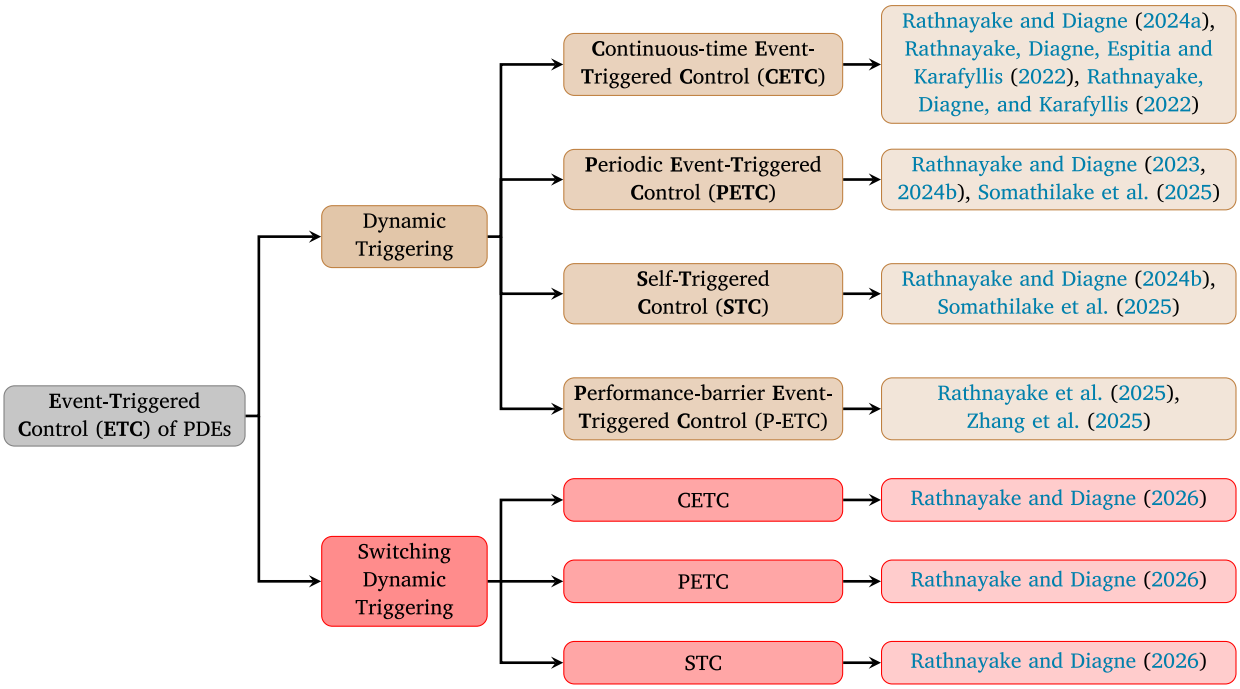

Fig. 2. Results on ETC of 1-D RD PDEs and 2 × 2 coupled hyperbolic PDEs.

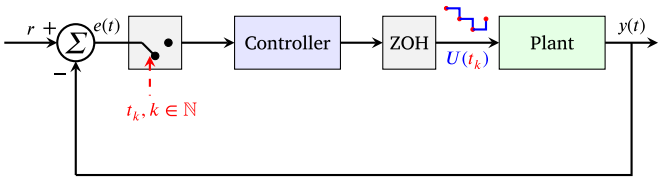

Fig. 3. Sampled-data control.

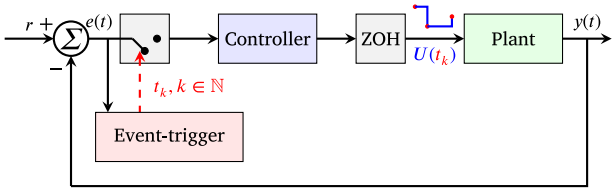

Fig. 4. Event-triggered control.

with $t_0 = 0$, where

$$\dot{m}(t) = f_d\Big(m(t), d^2(t), u[t]\Big).$$

The ETM ensures the following condition

$$d^2(t) \leq m(t), \forall t \in \big[0, \sup\{t_k\}_{k\in\mathbb{N}}\big),$$

$m(0) = m_0$ and f_d must be chosen s.t

$$m(t) > 0 \ \forall t \in \big[0, \sup\{t_k\}_{k\in\mathbb{N}}\big),$$

where the condition $m(t) > 0$ is required for a well-defined triggering condition.

The remainder of the paper focuses on the design of dynamic ETC for boundary regulation of the reach of an open channel flow, where enforcing piecewise-constant gate commands enhances controller feasibility and prolongs actuator lifetime. In irrigation networks, each gate movement requires mechanical motion, electrical power, and Supervisory Control and Data Acquisition (SCADA) coordination (Amin et al., 2013a, 2013b); therefore, reducing actuation frequency limits wear, lowers energy use, and diminishes maintenance demands. Less frequent adjustments also lead to smoother hydraulic transitions, mitigating oscillations and pressure surges associated with rapid gate motion. Hence, control strategies that achieve accurate flow regulation while minimizing gate activity offer clear advantages for sustainable and reliable operation.

3. Emulation of the continuous-time boundary control law of the Saint-Venant model

To design a continuous-time boundary control law for regulating water level in a hydraulic channel, it is advantageous to first use a physics-based model of the system. Considering the conservation of mass and momentum, the flow water in an open channel can be modeled by the Saint-Venant equations (Barré de Saint-Venant, 1871). In this work, we consider a prismatic open channel with an upstream gate that maintains a fixed inflow rate of water. Using a backstepping feedback law, our goal is to determine the downstream gate opening height that stabilizes the water level and velocity at a desired equilibrium set, and with respect to a given spatial norm. This system under consideration is illustrated in Fig. 5. In the following section, the Saint-Venant model is presented and the control problem is formulated.

3.1. Governing equations of the Saint-Venant model

Consider a one-dimensional prismatic open channel of unit width and length ℓ. For time $t \in [0, \infty)$ and longitudinal distance $x \in [0, \ell]$, let the water height be $H(x,t)$ and the depth-averaged water velocity be $V(x,t)$, then the Saint-Venant equations modeling the fluid flow are given by

$$H_t + (HV)_x = 0, \tag{1}$$

$$V_t + \left(\frac{V^2}{2} + gH\right)_x + \left(\frac{C_f V^2}{H} - gS_b\right) = 0, \tag{2}$$

where g is the constant acceleration of gravity, S_b is the constant bottom slope of the channel bed, C_f is the constant friction coefficient. Let $H_{eq} > 0$ and $V_{eq} > 0$ be the desired equilibrium states of $H(x,t)$

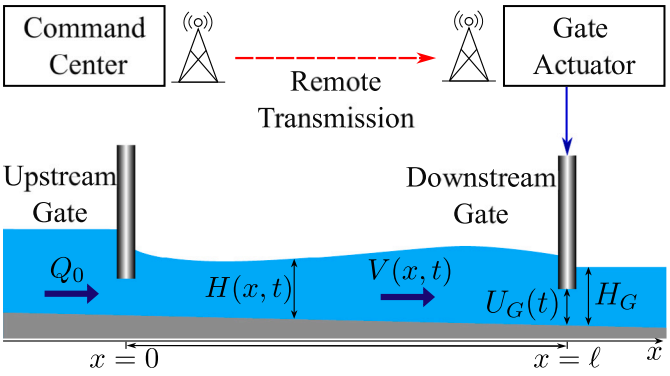

Fig. 5. Structure of the water canal.

and $V(x,t)$, respectively. Assume that the flow rate upstream is a known constant Q_0, and an underflow sluice gate is used at the downstream boundary (Swamee, 1992). Therefore, the following boundary conditions hold:

$$H(0,t)V(0,t) = Q_0, \tag{3}$$

$$H(\ell,t)V(\ell,t) = k_G\sqrt{2g}U_G(t)\sqrt{H(\ell,t)-H_G}, \tag{4}$$

the parameter k_G represents the constant discharge coefficient of the gate, H_G is the constant water level beyond the gate. The gate opening height, which serves as the control input for regulating the water level, is denoted by U_G. The values of the spatially distributed states $H(x,t)$ and $V(x,t)$, are measurable for all $x \in [0,\ell], t \in [0,\infty)$. Let the following assumptions hold for the desired equilibrium states.

Assumption 1. The following relationship holds between S_b, H_{eq}, and V_{eq}:

$$S_b = \frac{C_f V_{eq}^2}{gH_{eq}}.$$

Assumption 2. The following subcritical condition holds for the steady states of the system:

$$gH_{eq} > V_{eq}^2.$$

Let $\tilde{H}(x,t) = H(x,t) - H_{eq}$ and $\tilde{V}(x,t) = V(x,t) - V_{eq}$. Linearizing (1),(2) around the steady-state, the following expression holds:

$$\begin{pmatrix}\tilde{H}\\ \tilde{V}\end{pmatrix}_t + \begin{pmatrix}V_{eq} & H_{eq}\\ g & V_{eq}\end{pmatrix}\begin{pmatrix}\tilde{H}\\ \tilde{V}\end{pmatrix}_x + \begin{pmatrix}0 & 0\\ f_H & f_V\end{pmatrix}\begin{pmatrix}\tilde{H}\\ \tilde{V}\end{pmatrix} = \mathbf{0},$$

$$V_{eq}\tilde{H}(0,t) + H_{eq}\tilde{V}(0,t) = 0,$$

$$\left(\frac{Q_0}{2(H_{eq}-H_G)} - V_{eq}\right)\tilde{H}(\ell,t) - H_{eq}\tilde{V}(\ell,t) + k_G\sqrt{2g(H_{eq}-H_G)}\tilde{U}_G(t) = 0,$$

where f_V, f_H and $\tilde{U}_G(t)$ are defined as

$$f_H := -\frac{C_f V_{eq}^2}{H_{eq}^2}, \quad f_V := \frac{2C_f V_{eq}}{H_{eq}},$$

$$\tilde{U}_G(t) = U_G(t) - \frac{Q_0}{k_G\sqrt{2g(H_{eq}-H_G)}}.$$

Let us denote

$$M = \begin{pmatrix}V_{eq} & H_{eq}\\ g & V_{eq}\end{pmatrix}$$

The matrix M has two real distinct eigenvalues λ_1 and $-\lambda_2$ that satisfy

$$\lambda_1 = V_{eq} + \sqrt{gH_{eq}}, \quad -\lambda_2 = V_{eq} - \sqrt{gH_{eq}}.$$

Assumption 1 ensures that the equilibrium states H_{eq} and V_{eq} are constant, which in turn implies that λ_1 and λ_2 are also constant. Additionally, Assumption 2 guarantees that $\lambda_1, \lambda_2 > 0$. Subsequently, consider the following coordinate transformation:

$$\begin{pmatrix}u\\ v\end{pmatrix} = \begin{pmatrix}e^{\frac{\gamma_1}{\lambda_1}x} & 0\\ 0 & e^{-\frac{\gamma_2}{\lambda_2}x}\end{pmatrix}\begin{pmatrix}\sqrt{\frac{g}{H_{eq}}} & 1\\ -\sqrt{\frac{g}{H_{eq}}} & 1\end{pmatrix}\begin{pmatrix}\tilde{H}\\ \tilde{V}\end{pmatrix},$$

for

$$\gamma_1 = \frac{f_H}{2}\sqrt{\frac{H_{eq}}{g}} + \frac{f_V}{2}, \quad \gamma_2 = -\frac{f_H}{2}\sqrt{\frac{H_{eq}}{g}} + \frac{f_V}{2},$$

resulting in the following 2×2 linear hyperbolic PDE:

$$u_t(x,t) + \lambda_1 u_x(x,t) = c_1(x)v(x,t), \tag{5}$$

$$v_t(x,t) - \lambda_2 v_x(x,t) = c_2(x)u(x,t), \tag{6}$$

with boundary conditions,

$$u(0,t) = qv(0,t), \tag{7}$$

$$v(\ell,t) = \rho u(\ell,t) + U(t). \tag{8}$$

The terms $c_1(x)$, $c_2(x)$, q, ρ, and the control input determined by the control design, $U(t)$ are given by

$$c_1(x) = -\gamma_2 e^{\left(\frac{\gamma_1}{\lambda_1}+\frac{\gamma_2}{\lambda_2}\right)x}, \quad c_2(x) = -\gamma_1 e^{-\left(\frac{\gamma_1}{\lambda_1}+\frac{\gamma_2}{\lambda_2}\right)x},$$

$$q = -\frac{\lambda_2}{\lambda_1}, \quad \rho = \frac{Q_0 - 2\lambda_1(H_{eq}-H_G)}{Q_0 + 2\lambda_2(H_{eq}-H_G)}e^{-\left(\frac{\gamma_1}{\lambda_1}+\frac{\gamma_2}{\lambda_2}\right)\ell},$$

$$U(t) = \frac{2k_G g(2(H_{eq}-H_G))^{\frac{3}{2}}e^{-\frac{\gamma_2}{\lambda_2}\ell}}{\sqrt{H_{eq}}(Q_0 + 2\lambda_2(H_{eq}-H_G))}\tilde{U}_G(t).$$

In addition to Assumptions 1 and 2, we assume that the following condition holds for the boundary reflection terms ρ and q.

Assumption 3. The reflection terms in (7),(8) are assumed to satisfy the following condition:

$$|\rho q| < \frac{1}{\sqrt{2}}.$$

Assumption 3 ensures dissipative boundary conditions — a standard requirement for delay-robust boundary feedback design (Auriol & Di Meglio, 2020) — and is therefore adopted in the ETC designs presented in this contribution.

Remark 1. The control methodologies presented in the article are designed for general counter-convective 2×2 linear hyperbolic PDEs (5) and (6) with constant transport speeds and spatially varying in-domain coupling coefficients $c_1(x)$ and $c_2(x)$. The boundary conditions (7), (8) include both proximal (ρ) and distal ($q \neq 0$) reflection terms. Moreover, this article focuses on state-feedback control designs. The presented control mechanisms build upon (Somathilake et al., 2025; Zhang et al., 2025) for GEC results and Rathnayake and Diagne (2026) for GES results. The article (Zhang et al., 2025) considers a special case of the system (5)–(8) corresponding to the linearized Aw–Rascle–Zhang (ARZ) traffic model with $\rho = 0$. Note that if $\rho = 0$, Assumption 3 is satisfied for all q. Additionally, the derivations in Rathnayake and Diagne (2026), Somathilake et al. (2025) present observer-based designs. Accordingly, the derivations in Rathnayake and Diagne (2026), Somathilake et al. (2025), Zhang et al. (2025) have been adapted to align with the problem considered in this article.

Remark 2. Note that the PDE backstepping controller designed based on the linearized Saint-Venant model guarantees only local exponential stability of the nonlinear model (1)–(4), namely, when the initial condition is sufficiently close to the desired equilibrium. To address a wider

operating range, a multi-model design based on several Linear Time-Invariant (LTI) models defined around different operating points was proposed in Martins et al. (2012), where an internal-model boundary control design was employed to guarantee exponential stability. By combining multiple local models, this approach can better capture the dynamics of the underlying nonlinear system over a wider operating range. Moreover, a conceptual parallel can be drawn between this multi-model approach and the event-triggered gain-scheduling framework in Espitia and Auriol (2025), as both employ locally appropriate controller designs to accommodate variations in the operating conditions. The multi-model concept could, in principle, also be integrated with the backstepping design considered here and may provide a natural avenue for extending the proposed framework beyond a single operating point. Such an extension, however, is outside the scope of the present work, which is focused specifically on the development of new ETMs for deterministic and unperturbed coupled linear hyperbolic PDEs.

In the following section, we present the CTC design, which serves as a basis for the emulation-based ETC control strategies developed in this article.

3.2. Continuous-time controller design

The CTC design is based on the framework presented in Vazquez et al. (2011). Initially, consider the following backstepping transformation and its inverse:

$$\begin{aligned}\alpha(x,t) =&u(x,t) - \int_0^x K^{11}(x,\xi)u(\xi,t)d\xi\\ &- \int_0^x K^{12}(x,\xi)v(\xi,t)d\xi,\\ \beta(x,t) =&v(x,t) - \int_0^x K^{21}(x,\xi)u(\xi,t)d\xi\\ &- \int_0^x K^{22}(x,\xi)v(\xi,t)d\xi,\end{aligned}$$

$$\begin{aligned}u(x,t) =& \alpha(x,t)+ \int_0^x L^{11}(x,\xi)\alpha(\xi,t)d\xi\\ &+ \int_0^x L^{12}(x,\xi)\beta(\xi,t)d\xi,\\ v(x,t) =& \beta(x,t)+ \int_0^x L^{21}(x,\xi)\alpha(\xi,t)d\xi\\ &+ \int_0^x L^{22}(x,\xi)\beta(\xi,t)d\xi,\end{aligned}$$

where $K^{ij}(x,\xi)$ and $L^{ij}(x,\xi)$, $i,j = 1,2$ are the gain functions and the inverse gain functions, respectively, both defined in the triangular domain $\mathcal{T} = \{(x,\xi) : 0 \le \xi \le x \le \ell\}$. The reader is referred to Vazquez et al. (2011) for the defining PDEs that govern the kernels $K^{ij}(x,\xi)$ and $L^{ij}(x,\xi)$, $i,j = 1,2$. Evaluating the time and spatial derivatives of the forward transformation and accounting for the boundary conditions, one finds that the continuous-time boundary control law given by

$$\begin{aligned}U(t) =& \int_0^\ell \left(N_u(\xi)u(\xi,t) + N_v(\xi)v(\xi,t)\right)d\xi, \qquad (9)\\ N_u(\xi) =& K^{21}(\ell,\xi) - \rho K^{11}(\ell,\xi),\\ N_v(\xi) =& K^{22}(\ell,\xi) - \rho K^{12}(\ell,\xi),\end{aligned}$$

that can be expressed as

$$\begin{aligned}U(t) =& \int_0^\ell \left(N_\alpha(\xi)\alpha(\xi,t) + N_\beta(\xi)\beta(\xi,t)\right)d\xi, \qquad (10)\\ N_\alpha(\xi) =& L^{21}(\ell,\xi) - \rho L^{11}(\ell,\xi),\\ N_\beta(\xi) =& L^{22}(\ell,\xi) - \rho L^{12}(\ell,\xi),\end{aligned}$$

maps the system (5)–(8) into the following target system

$$\alpha_t(x,t) + \lambda_1\alpha_x(x,t) = 0, \qquad (11)$$

$$\beta_t(x,t) - \lambda_2\beta_x(x,t) = 0, \qquad (12)$$

$$\alpha(0,t) = q\beta(0,t), \qquad (13)$$

$$\beta(\ell,t) = \rho\alpha(\ell,t). \qquad (14)$$

As mentioned earlier, the ETC designs presented in this article are emulation based; that is, the control input is determined by sampling the CTC signal (10), at each event. The following section formally states the emulation framework considered and outlines several key properties associated with it.

3.3. Emulation of the PDE backstepping control

Our ETC design is based on the emulation of the exponentially stabilizing feedback law (9). Therefore, we sample the input $U(t)$ at time instants $\{t_k\}_{k\in\mathbb{N}}$ scheduled through an event-triggered rule. For $t \in [t_k, t_{k+1})$, $k \in \mathbb{N}$, consider the control input

$$U_k := U(t_k). \qquad (15)$$

From (8), the following holds

$$v(\ell,t) = \rho u(\ell,t) + U_k. \qquad (16)$$

A crucial variable of interest is *input holding error*, $d(t)$. That is the deviation of the sampled input relative to its continuous-time counterpart. For $t \in [t_k, t_{k+1})$, $k \in \mathbb{N}$:

$$d(t) := U_k - U(t). \qquad (17)$$

Note that we have expressed $d(t)$ in terms of the target system states (α,β), which leads to the following system, where the input holding error appears at the controlled boundary

$$\alpha_t(x,t) + \lambda_1\alpha_x(x,t) = 0, \qquad (18)$$

$$\beta_t(x,t) - \lambda_2\beta_x(x,t) = 0, \qquad (19)$$

$$\alpha(0,t) = q\beta(0,t), \qquad (20)$$

$$\beta(\ell,t) = \rho\alpha(\ell,t) + d(t). \qquad (21)$$

The closed-loop system (5)–(7),(15),(16) is well-posed between two sampling instants as established in Espitia et al. (2020) and restated below.

Proposition 1 (*Well-Posedness*). *For given states at time t_k, $\left(u[t_k], v[t_k]\right)^T \in L^2\left((0,\ell);\mathbb{R}^2\right)$, there exists a unique solution $(u,v)^T \in C^0\left([t_k,t_{k+1}]; L^2\left((0,\ell);\mathbb{R}^2\right)\right)$ to the system (5)–(7),(15),(16), between two time instants t_k and t_{k+1} for each $k \in \mathbb{N}$.*

Proof. Consider an event time $t_k, k \in \mathbb{N}$ with states $\left(u[t_k], v[t_k]\right)^T \in L^2\left((0,\ell);\mathbb{R}^2\right)$. The system (5)–(7),(15),(16) is affected by piecewise-constant boundary inputs, hence using Davó et al. (2019, Appendix) along with the notion of solution adopted in Prieur et al. (2014), there exists a unique weak solution $(u,v)^T \in C^0\left([t_k,t_{k+1}]; L^2\left((0,\ell);\mathbb{R}^2\right)\right)$ to the system (5)–(7),(15),(16) between two time instants t_k and t_{k+1} for each $k \in \mathbb{N}$.

The following lemma provides an estimate on the growth rate of the input-holding error $d(t)$, which is instrumental for deriving the subsequent triggering conditions.

Lemma 1. *The following expression holds for the input holding error defined in (17):*

$$(\dot{d}(t))^2 \le \varepsilon_0 d^2(t) + \varepsilon_1\|\alpha[t]\|^2 + \varepsilon_2\|\beta[t]\|^2 + \varepsilon_3\alpha(\ell,t)^2, \qquad (22)$$

along the solution of (18)–(21) for all $t \in (t_k,t_{k+1}), k \in \mathbb{N}$ where $\varepsilon_0,\varepsilon_1,\varepsilon_2,\varepsilon_3 > 0$ are given by

$$\varepsilon_0 = 4(\lambda_2 N_\beta(\ell))^2, \qquad (23)$$

$$\varepsilon_1 = 4\lambda_1^2 \int_0^\ell (N'_\alpha(\xi))^2 d\xi, \tag{24}$$

$$\varepsilon_2 = 4\lambda_2^2 \int_0^\ell (N'_\beta(\xi))^2 d\xi, \tag{25}$$

$$\varepsilon_3 = 4(\lambda_1 N_\alpha(\ell) - \lambda_2 \rho N_\beta(\ell))^2. \tag{26}$$

Proof. Taking the time derivative of (17) for $t \in (t_k, t_{k+1}), k \in \mathbb{N}$, and using (18)–(21), the following expression holds:

$$\dot{d}(t) = -\lambda_2 N_\beta(\ell) d(t) + (\lambda_1 N_\alpha(\ell) - \lambda_2 \rho N_\beta(\ell))\alpha(\ell, t) - \int_0^\ell \left(\lambda_1 N'_\alpha(\xi)\alpha(\xi,t) - \lambda_2 N'_\beta(\xi)\beta(\xi,t)\right) d\xi.$$

Subsequently, taking the square, using Young's inequality and Cauchy–Schwarz inequality, (22) can be obtained.

In addition, the following lemma provides an estimate on $d(t)^2$ for $t \in [t_k, t_{k+1}), k \in \mathbb{N}$ along the solution of (18)–(21) evaluated at $t = t_k$. This result is required for the derivation of the STC methodologies presented later in this paper.

Lemma 2. *The following expression holds for the input holding error defined in (17):*

$$d(t)^2 \le F(t_k) e^{\varrho^\star (t - t_k)}, \tag{27}$$

along the solution of (18)–(21) for all $t \in [t_k, t_{k+1}), k \in \mathbb{N}$ where

$$F(t) = 3\varrho \int_0^\ell \left(\frac{1}{\lambda_1} \alpha(x,t)^2 e^{-\bar{\mu}\frac{x}{\lambda_1}} + \frac{q^2}{\lambda_2} \beta(x,t)^2 e^{\bar{\mu}\frac{x}{\lambda_2}} \right) dx, \tag{28}$$

$$\bar{\mu} \in \left(0, \frac{2\lambda_1\lambda_2}{\ell(\lambda_1+\lambda_2)} \ln\left(\frac{1}{\sqrt{2}|\rho q|}\right)\right], \tag{29}$$

$$\varrho^\star = 2q^2 \varrho e^{\frac{\bar{\mu}\ell}{\lambda_2}}, \tag{30}$$

$$\varrho = 4 \max\left\{ \lambda_1 e^{\frac{\bar{\mu}\ell}{\lambda_1}} \int_0^\ell N_\alpha(\xi)^2 d\xi, \frac{\lambda_2}{q^2} \int_0^\ell N_\beta(\xi)^2 d\xi \right\}. \tag{31}$$

Proof. For $\bar{\mu}$ in (29), define $\bar{V}_1(t)$ as

$$\bar{V}_1(t) := \int_0^\ell \left(\frac{1}{\lambda_1} \alpha(x,t)^2 e^{-\bar{\mu}\frac{x}{\lambda_1}} + \frac{q^2}{\lambda_2} \beta(x,t)^2 e^{\bar{\mu}\frac{x}{\lambda_2}} \right) dx.$$

Taking the derivative of $\bar{V}_1(t)$ along the solution of (18)–(21) for all $t \in [t_k, t_{k+1}), k \in \mathbb{N}$, the following bound holds:

$$\dot{\bar{V}}_1(t) \le -\bar{\mu}\bar{V}(t) + 2q^2 e^{\bar{\mu}\frac{\ell}{\lambda_2}} d(t)^2,$$

additionally, squaring (17) and using Young's inequality and Cauchy–Schwarz inequality $d(t)^2$ can be bounded as

$$d(t)^2 \le \varrho \bar{V}_1(t_k) + \varrho \bar{V}_1(t),$$

for ϱ satisfying (31). Therefore, using the comparison principle we can directly obtain (27).

In the subsequent sections, we present the triggering conditions that determine the times at which the control input is sampled to emulate of the CTC signal $U(t)$. Initially, we state the class of dynamic triggering conditions termed *regular* ETC (R-ETC) (Espitia et al., 2018, 2020; Rathnayake, Diagne, Espitia & Karafyllis, 2022).

4. Regular event-triggered control

Now that we have established the well-posedness of the sampled-data boundary control, we will devote the present part of our developments to the design of *regular* ETC (R-ETC) by introducing three schemes: continuous-time event-triggered (R-CETC), periodic event-triggered (R-PETC), and self-triggered control (R-STC). Hereafter, we will present ETMs without insisting on complex proof strategies that are already reported in the literature. Our R-ETC schemes follow the results in Somathilake et al. (2025), adapted as necessary to fit the framework considered in this work.

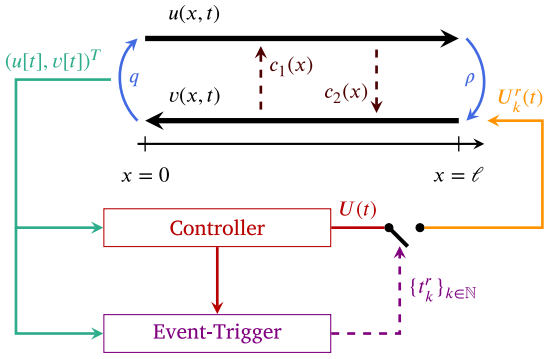

Fig. 6. R-CETC with dynamic triggering.

4.1. Continuous-time event-triggered control

We present an ETC design in which the control input is updated at discrete event times, while a triggering condition is continuously monitored to determine the occurrence of these events. A schematic of the resulting closed-loop system is given in Fig. 6, where the input signal is updated following a dynamic ETM.

Let $I^r = \{t_k^r\}_{k\in\mathbb{N}}$ denote the increasing sequence of event times associated with R-CETC, and it consists of two parts:

1. An ETC input U_k^r

$$U_k^r := U(t_k^r), \tag{32}$$

for $t \in \left[t_k^r, t_{k+1}^r\right), k \in \mathbb{N}$, where $U(t)$ is given by (9). Then, the boundary condition (16) becomes

$$v(\ell, t) = \rho u(\ell, t) + U_k^r. \tag{33}$$

2. A continuous-time ETM determining event times

$$t_{k+1}^r = \inf\left\{t \in \mathbb{R}_{>0} \mid t > t_k^r, \Gamma^r(t) > 0, k \in \mathbb{N}\right\}, \tag{34}$$

with $t_0^r = 0$, where $\Gamma^r(t)$ is the triggering function defined as

$$\Gamma^r(t) := d(t)^2 - \theta m^r(t). \tag{35}$$

The function $d(t)$ is given by (17) for $t \in \left[t_k^r, t_{k+1}^r\right), k \in \mathbb{N}$, and $m^r(t)$ satisfies the ODE

$$\dot{m}^r(t) = -\eta m^r(t) - \theta_m d(t)^2 + \kappa_{1,1}\|\alpha[t]\|^2 + \kappa_{1,2}\|\beta[t]\|^2 + \kappa_{1,3}\alpha(\ell, t)^2, \tag{36}$$

for $t \in \left(t_k^r, t_{k+1}^r\right), k \in \mathbb{N}$ with $m^r\left(t_0^r\right) = m^r(0) > 0$ and $m^r\left(t_k^{r-}\right) = m^r\left(t_k^r\right)$. The parameters $\theta, \eta, \theta_m, \kappa_{1,1}, \kappa_{1,2}, \kappa_{1,3} > 0$ are event-trigger parameters to be appropriately chosen.

Note that at each event, the input holding error, $d(t_k^r) = 0, k \in \mathbb{N}$. Then, for $t \in [t_k^r, t_{k+1}^r)$, as $d(t)$ grows relative to the state-dependent threshold, the trigger may reach zero resulting in $\Gamma^r((t_{k+1}^r)^-) = 0$ and leading to an event at $t = t_{k+1}^r$. This evolution of the dynamic variable $m^r(t)$ alongside $d(t)^2$ is illustrated in Fig. 7.

The parameter selection guideline for R-CETC are defined below.

Definition 1. The parameters $\theta, \eta > 0$ are arbitrary design parameters, and $\kappa_{1,1}, \kappa_{1,2}, \kappa_{1,3} > 0$ are chosen as

$$\kappa_{1,1} = \frac{\varepsilon_1}{\theta(1-\sigma)}, \quad \kappa_{1,2} = \frac{\varepsilon_2}{\theta(1-\sigma)}, \quad \kappa_{1,3} = \frac{\varepsilon_3}{\theta(1-\sigma)}, \tag{37}$$

where $\sigma \in (0, 1)$ and $\varepsilon_1, \varepsilon_2, \varepsilon_3$ are given by (24)–(26). The event-trigger parameter $\theta_m > 0$ is chosen as

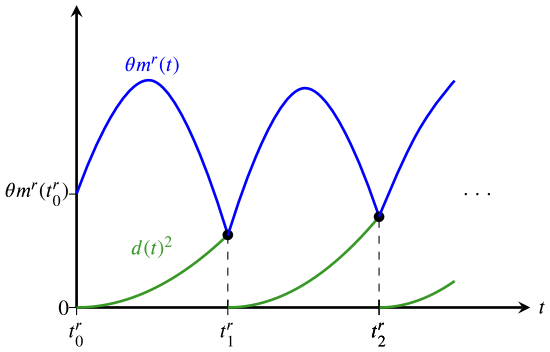

Fig. 7. Schematic of the evolution of the dynamic variable $m^r(t)$ alongside $d(t)^2$ under R-CETC.

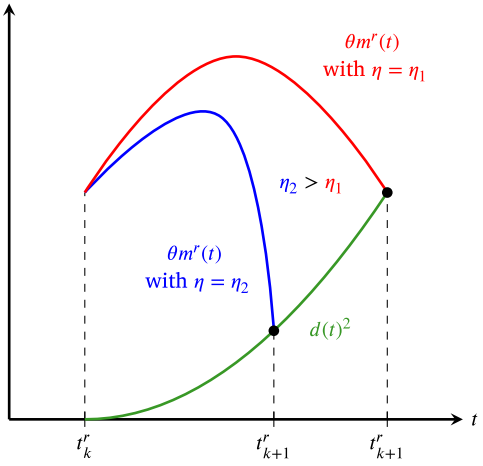

Fig. 8. Schematic of the evolution of the dwell-time according to the ETM for $\eta_1 < \eta_2$.

$$\theta_m = 2Aq^2 e^{\mu \frac{\ell}{\lambda_2}}, \tag{38}$$

where

$$\mu \in \left(0, \frac{2\lambda_1\lambda_2}{\ell(\lambda_1+\lambda_2)} \ln\left(\frac{1}{\sqrt{2}|\rho q|}\right)\right), \tag{39}$$

$$A > \max\left\{\frac{\kappa_{1,3} e^{\mu\frac{\ell}{\lambda_1}}}{1-2\rho^2 q^2 e^{\mu\left(\frac{\ell}{\lambda_1}+\frac{\ell}{\lambda_2}\right)}}, \frac{\max\{\kappa_{1,1},\kappa_{1,2}\}r}{\mu}\right\}, \tag{40}$$

$$r := \frac{1}{\min\left\{\frac{1}{\lambda_1} e^{-\mu\frac{\ell}{\lambda_1}}, \frac{q^2}{\lambda_2}\right\}}. \tag{41}$$

Remark 3. For system (5)–(7),(32)–(36), the parameters of ETM are selected following Definition 1. The parameters $\kappa_{1,1}, \kappa_{1,2}, \kappa_{1,3} > 0$ play a role in *excluding Zeno behavior*, $\theta_m > 0$ ensures GEC, while the constants $\eta, \theta > 0$ are *free parameters*. The triggering rule is conceptually illustrated by Fig. 8. The smaller the η, the larger the time it takes for $d^2(t)$ to equate $\theta m^r(t)$ (see (35)), leading to larger dwell-times.

Next, we state the GEC of the equilibrium of the closed-loop system under R-CETC.

Theorem 1 (*Results under R-CETC*). *Let $I^r = \{t_k^r\}_{k\in\mathbb{N}}$ with $t_0^r = 0$ be the set of event times generated by the R-CETC approach (32)–(36) with appropriate choices for the event-trigger parameters under Definition 1. Then, it holds that*

$$I^r(t) \le 0, \forall t \in [0, \sup(I^r)). \tag{42}$$

As a result, the following results hold:

R1: The set of event times I^r generates an increasing sequence. It holds that $t_{k+1}^r - t_k^r \ge \tau_1 > 0, k \in \mathbb{N}$, where

$$\tau_1 = \frac{1}{a}\ln\left(1 + \frac{\sigma a}{(1-\sigma)(a+\theta\theta_m)}\right), \tag{43}$$

for $\sigma \in (0,1)$. Here, $a > 0$ is given by

$$a = 1 + \varepsilon_0 + \eta, \tag{44}$$

for ε_0 defined in (23). Due to the existence of a uniform positive MDT $\tau_1 > 0$, it follows that $t_k^r \to \infty$ as $k \to \infty$, thereby guaranteeing Zeno-free behavior.

R2: For every $(u[0], v[0])^T \in L^2\left((0,\ell);\mathbb{R}^2\right)$, there exists a unique solution $(u,v)^T \in C^0\left(\mathbb{R}_+; L^2\left((0,\ell);\mathbb{R}^2\right)\right)$ to the system (5)–(7),(32)–(36) for all $t > 0$.

R3: The dynamic variable $m^r(t)$ governed by (36) with $m^r(0) > 0$ satisfies $m^r(t) > 0$ for all $t > 0$.

R4: Consider a Lyapunov candidate

$$V^r(t) = V_1(t) + m^r(t), \tag{45}$$

where

$$V_1(t) := \int_0^\ell \left(\frac{A}{\lambda_1}\alpha(x,t)^2 e^{-\mu\frac{x}{\lambda_1}} + \frac{Aq^2}{\lambda_2}\beta(x,t)^2 e^{\mu\frac{x}{\lambda_2}}\right) dx. \tag{46}$$

Then, it holds that

$$\dot{V}^r(t) \le -a^\star V^r(t), \tag{47}$$

for all $t \in (t_k^r, t_{k+1}^r), k \in \mathbb{N}$, and

$$V^r(t) \le e^{-a^\star t} V^r(0), \tag{48}$$

for all $t > 0$, where

$$a^\star := \min\left\{\mu - \frac{\max\{\kappa_{1,1},\kappa_{1,2}\}r}{A}, \eta\right\} > 0. \tag{49}$$

See Definition 1 for details on $\mu, \kappa_{1,1}, \kappa_{1,2}, r, A, \eta > 0$.

R5: The closed-loop signal $\|u[t]\| + \|v[t]\|$ associated with the solution of the system (5)–(7),(32)–(36), exponentially converges to zero. Specifically, the following relationship holds:

$$\|u[t]\| + \|v[t]\| \le M_a e^{-\frac{a^\star}{2}t}\left(\|u[0]\| + \|v[0]\| + \underbrace{m^r(0)^{\frac{1}{2}}}_{GEC}\right),$$

for all $t > 0$ and some constant $M_a > 0$.

The existence of a minimum dwell-time in R1 is ensured by the choice of $\kappa_{1,1}, \kappa_{1,2}, \kappa_{1,3}$ as specified in (37), which, in conjunction with Proposition 1, yields result R2. The result R3 is a direct consequence of the triggering condition (34)–(36). Finally, utilizing R2, R3, and the Lyapunov function candidate (45), the results R4 and R5 can be shown given that the triggering parameters are selected as in Definition 1. The proof of Theorem 1 follows reasoning similar to that used in the proof of Proposition 3 of Somathilake et al. (2025).

In what follows, we introduce a PETC scheme that is obtained by modifying the R-CETC scheme appropriately.

4.2. Periodic event-triggered control

We present an ETC design in which the control input is updated at discrete event times; however, in contrast to the R-CETC approach, the triggering condition is evaluated only periodically. This is achieved by introducing a new triggering condition that is checked periodically while still ensuring that the triggering condition of the R-CETC scheme is satisfied. A schematic of the resulting closed-loop system under R-PETC is given in Fig. 9.

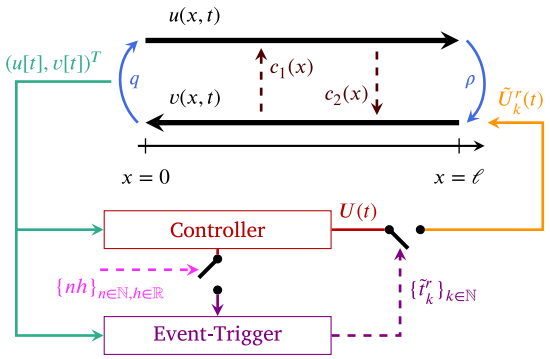

Fig. 9. R-PETC with dynamic triggering.

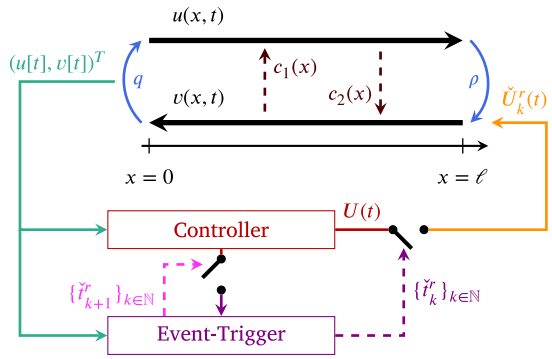

Fig. 10. R-STC with dynamic triggering.

Let $\tilde{I}^r = \{\tilde{t}^r_k\}_{k\in\mathbb{N}}$ denote the sequence of event times associated with R-PETC, and let the event-trigger parameters $\theta, \eta, \theta_m, \kappa_{1,1}, \kappa_{1,2}, \kappa_{1,3} > 0$ be selected as outlined in Definition 1. The R-PETC strategy consists of two parts:

1. An ETC input $\tilde{U}^r_k$

$$\tilde{U}^r_k := U(\tilde{t}^r_k), \tag{50}$$

for $t \in \left[\tilde{t}^r_k, \tilde{t}^r_{k+1}\right), k \in \mathbb{N}$, where $U(t)$ is given by (9). Then, the boundary condition (16) becomes

$$v(\ell, t) = \rho u(\ell, t) + \tilde{U}^r_k. \tag{51}$$

2. A periodic ETM determining event times

$$\tilde{t}^r_{k+1} = \inf\{t \in \mathbb{R}_+ \,|t > \tilde{t}^r_k, \tilde{\Gamma}^r(t) > 0, t = nh_1, \\ h_1 > 0, n \in \mathbb{N}, k \in \mathbb{N}\}, \tag{52}$$

with $\tilde{t}^r_0 = 0$. Here h_1 is the sampling period selected as

$$0 < h_1 \leq \tau_1, \tag{53}$$

where τ_1 is given by (43), and $\tilde{\Gamma}^r(t)$ is the triggering function defined as

$$\tilde{\Gamma}^r(t) := (a + \theta\theta_m)e^{ah_1} d^2(t) - \theta\theta_m d^2(t) - \theta a m^r(t), \tag{54}$$

where a is defined in (44). Further, $d(t)$ is defined in (17), and $m^r(t)$ satisfies the ODE given by (36), along the solution of (18)–(21) for all $t \in \left(\tilde{t}^r_k, \tilde{t}^r_{k+1}\right), k \in \mathbb{N}$.

The R-CETC in (34)–(36) differs from the R-PETC in (52)–(54) through the redesign of the triggering function, where $\Gamma^r(t)$ is replaced by $\tilde{\Gamma}^r(t)$, leading to periodic rather than continuous evaluation.

Next, we state the GEC of the equilibrium of the closed-loop system under R-PETC.

Theorem 2 (*Results under R-PETC*). *Let $\tilde{I}^r = \{\tilde{t}^r_k\}_{k\in\mathbb{N}}$ with $\tilde{t}^r_0 = 0$ be the set of event times generated by the R-PETC approach (50)–(54) with appropriate choices for the event-trigger parameters under Definition 1. Then, the following results hold:*

- *R1: For every $(u[0], v[0])^T \in L^2\left((0,\ell);\mathbb{R}^2\right)$, there exists a unique solution $(u, v)^T \in C^0\left(\mathbb{R}_+; L^2\left((0,\ell);\mathbb{R}^2\right)\right)$ to the R-PETC closed-loop system (5)–(7),(50)–(54) for all $t > 0$.*
- *R2: $\Gamma^r(t)$ given by (35) satisfies $\Gamma^r(t) \leq 0$ for all $t > 0$, along the R-PETC closed-loop solution.*
- *R3: The dynamic variable $m^r(t)$ governed by (36) with $m^r(0) > 0$ satisfies $m^r(t) > 0$ for all $t > 0$, along the R-PETC closed-loop solution.*
- *R4: The Lyapunov candidate $V^r(t)$ given by (45),(46) satisfies (47),(49) for all $t \in (\tilde{t}^r_k, \tilde{t}^r_{k+1}), k \in \mathbb{N}$ and (48)–(49) for all $t > 0$, along the R-PETC closed-loop solution.*
- *R5: The closed-loop signal $\|u[t]\| + \|v[t]\|$ associated with the solution of the system (5)–(7),(50)–(54) exponentially converges to zero. Specifically, the following relationship holds:*

$$\|u[t]\| + \|v[t]\| \leq M_a e^{-\frac{a^\star}{2}t}\left(\|u[0]\| + \|v[0]\| + \underbrace{m^r(0)^{\frac{1}{2}}}_{GEC}\right),$$

for all $t > 0$ and some constant $M_a > 0$.

Since the triggering function is evaluated periodically under R-PETC, Zeno phenomenon is inherently excluded and the set of event times $\tilde{I}^r$ generates an increasing sequence. Then, together with Proposition 1, result R1 follows. The triggering function $\tilde{\Gamma}^r(t)$ is designed such that if $\tilde{\Gamma}^r(nh_1) \leq 0$ for any $n \in [\tilde{t}^r_k/h_1, \tilde{t}^r_{k+1}/h_1) \cap \mathbb{N}, k \in \mathbb{N}$, $\Gamma^r(t) \leq 0$ for all $t \in [nh_1, (n+1)h_1)$. Therefore, even if $\tilde{\Gamma}^r(t)$ is evaluated periodically as in (54), $\Gamma^r(t) \leq 0$ for $t \in [\tilde{t}^r_k, \tilde{t}^r_{k+1}), k \in \mathbb{N}$. Hence, the ETM (34),(35) is satisfied for all $t \geq 0$ and the results in Theorem 1 hold under R-PETC. The proof of Theorem 2 follows reasoning similar to that used in the proof of Theorem 1 in Somathilake et al. (2025).

In what follows, we introduce a STC scheme that is obtained by modifying the R-CETC scheme appropriately.

4.3. Self-triggered control

In this subsection, we present an ETC design in which the control input is updated at discrete event times. In contrast to the R-CETC approach, the next event time is determined at the current event. This is achieved by leveraging prediction of the input holding error provided in Lemma 2, while still ensuring that the triggering condition of the R-CETC scheme is satisfied. A schematic of the resulting closed-loop system under R-STC is given in Fig. 10.

Let $\check{I}^r = \{\check{t}^r_k\}_{k\in\mathbb{N}}$ denote the sequence of event times associated with R-STC. Let the event-trigger parameters $\theta, \eta, \theta_m, \kappa_{1,1}, \kappa_{1,2}, \kappa_{1,3} > 0$ be selected as outlined in Definition 1. The R-STC strategy consists of two parts:

1. An ETC input $\check{U}^r_k$

$$\check{U}^r_k := U(\check{t}^r_k), \tag{55}$$

for $t \in \left[\check{t}^r_k, \check{t}^r_{k+1}\right), k \in \mathbb{N}$ where $U(t)$ is given by (9). Then, the boundary condition (16) becomes

$$v(\ell, t) = \rho u(\ell, t) + \check{U}^r_k. \tag{56}$$

2. A self-trigger determining event times

$$\check{t}^r_{k+1} = \check{t}^r_k + G^r\left(F(\check{t}^r_k), m^r\left(\check{t}^r_k\right)\right), \tag{57}$$

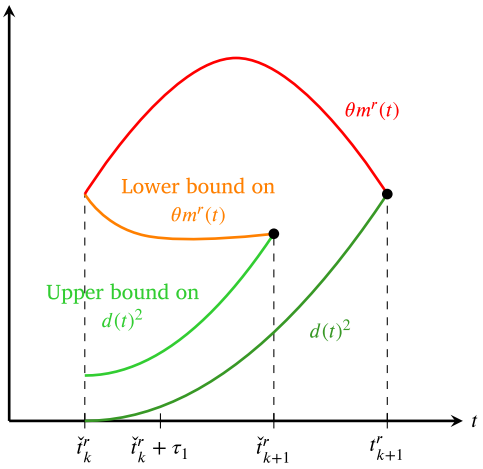

Fig. 11. Evolution of the dwell-time according to the ETM for R-STC.

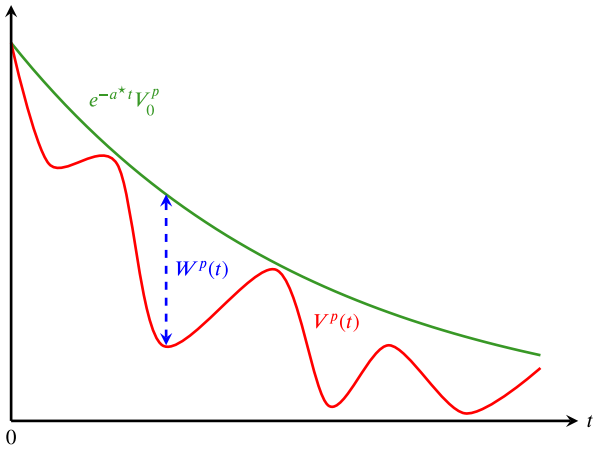

Fig. 12. Performance-barrier: $V^p(t)$ has the flexibility to increase and $W^p(t)$ is the performance residual allowing positive $\dot{V}^p(t)$.

with $\check{t}_0^r = 0$ and $G^r(\cdot,\cdot) > 0$ is a positive function uniformly bounded away from zero

$$G^r\left(F(t), m^r(t)\right) := \max\left\{\tau_1, \frac{1}{\varrho^\star + \eta}\ln\left(\frac{\theta m^r(t) + \frac{\theta\theta_m F(t)}{\varrho^\star+\eta}}{F(t) + \frac{\theta\theta_m F(t)}{\varrho^\star+\eta}}\right)\right\}. \tag{58}$$

Here, τ_1 is R-CETC MDT given by (43), $m^r(t)$ satisfies the dynamics (36) along the solution of (18)–(21) for $t \in \left(\check{t}_k^r, \check{t}_{k+1}^r\right), k \in \mathbb{N}$. The constant $\varrho^\star > 0$ is defined in (30) and $F(t)$ is defined in (28).

Remark 4. The ETM is designed using the positively lower-bounded function $G(\cdot,\cdot)$ defined in (58) to guarantee that $\Gamma^r(t)$ given by (35) and associated with R-CETC remains non-positive along the solution of R-STC closed-loop system for all $t \in \left[\check{t}_k^r, \check{t}_{k+1}^r\right), k \in \mathbb{N}$. This requires finding an upper bound for $d(t)^2$ and lower bound for $m^r(t)$, which are the constituent terms of the R-CETC triggering function $\Gamma^r(t)$. Hence, as we assume that upper bound for $d(t)^2$ and lower bound for $m^r(t)$ become equal at a unique $t_k^\star \geq \check{t}_k^r + \tau_1$, it becomes guaranteed that $d(t)^2 \leq \theta m^r(t)$, that is $\Gamma^r(t) \leq 0$, which is consistent with R-CETC. If $t_k^\star < \tau_1$, the filter in (58) generates an event at the MDT. An illustration is depicted in Fig. 11.

Next, we state the GEC of the equilibrium of the closed-loop system under R-STC.

Theorem 3 (*Results under R-STC*). *Let $\check{I}^r = \{\check{t}_k^r\}_{k\in\mathbb{N}}$ with $\check{t}_0^r = 0$ be the set of event times generated by the R-STC approach (55)–(58) with appropriate choices for the event-trigger parameters under Definition 1. Then, the following results hold:*

- *R1: For every $(u[0], v[0])^T \in L^2\left((0,\ell);\mathbb{R}^2\right)$, there exists a unique solution $(u,v)^T \in C^0\left(\mathbb{R}_+; L^2\left((0,\ell);\mathbb{R}^2\right)\right)$ to the R-STC closed-loop system (5)–(7),(55)–(58) for all $t > 0$.*
- *R2: $\Gamma^r(t)$ given by (35) satisfies $\Gamma^r(t) \leq 0$ for all $t > 0$, along the R-STC closed-loop solution.*
- *R3: The dynamic variable $m^r(t)$ governed by (36) with $m^r(0) > 0$ satisfies $m^r(t) > 0$ for all $t > 0$, along the R-STC closed-loop solution.*
- *R4: The Lyapunov candidate $V^r(t)$ given by (45),(46) satisfies (47),(49) for all $t \in (\check{t}_k^r, \check{t}_{k+1}^r), k \in \mathbb{N}$ and (48)–(49) for all $t > 0$, along the R-STC closed-loop solution.*
- *R5: The closed-loop signal $\|u[t]\| + \|v[t]\|$ associated with the solution of the system (5)–(7),(55)–(58) exponentially converges to zero. Specifically, the following relationship holds:*

$$\|u[t]\| + \|v[t]\| \leq M_a e^{-\frac{a^\star}{2}t}\left(\|u[0]\| + \|v[0]\| + \underbrace{m^r(0)^{\frac{1}{2}}}_{GEC}\right),$$

for all $t > 0$ and some constant $M_a > 0$.

The set of event times $\check{I}^r$ forms an increasing sequence, since the Zeno phenomenon is excluded by the triggering condition (57). Subsequently, by invoking Proposition 1, result R1 can be established. Results R2 and R3 can be shown using Lemma 2 and the triggering condition (57),(58). Subsequently R4 and R5 follow since the triggering condition (34),(35) is satisfied for all $t > 0$ and the results in Theorem 1 holds under R-STC. The proof of Theorem 3 follows reasoning similar to that used in the proof of Theorem 2 in Somathilake et al. (2025).

Now that we have introduced the R-ETC methods, we move on to modifying these triggering conditions by incorporating a performance-barrier that allows for greater dwell-times.

5. Performance-barrier event-triggered control

We employ a P-ETC to stabilize the same class of systems. As illustrated in Fig. 12, the concept of *performance-barrier*, inspired by safety-critical control (Ames et al., 2019, 2017; Krstić, 2024; Taylor et al., 2021), refers to a nominal Lyapunov decrease viewed as a threshold not to be violated. In R-CETC, R-PETC and R-STC, event-triggers enforce monotonic decay by ensuring the Lyapunov derivative stays negative, making it decrease faster than a reference exponential $e^{-a^\star t}V_0^p$, which is called the *performance-barrier*. The idea of P-ETC is to relax the monotonicity while still respecting this barrier, yielding longer dwell-times and fewer updates, as in Ong and Cortés (2024) for ODEs.

By appropriately augmenting the triggering conditions stated in Section 4 with the performance-barrier, we present continuous-time event-triggered control (P-CETC), periodic event-triggered control (P-PETC), and self-triggered control (P-STC) schemes within the P-ETC framework. The P-ETC schemes presented here are adapted from Zhang et al. (2025) where the system considered has $\rho = 0$, which makes Assumption 3 trivially satisfied, as explained in Remark 1. Consequently, (39) is satisfied for any $\mu > 0$. For the general case with $\rho \neq 0$, the performance barrier synthesis from Zhang et al. (2025) carries over, provided Assumption 3 is satisfied to account for the boundary term ρ, thereby guaranteeing the existence of $\mu > 0$ satisfying (39).

5.1. Performance-barrier continuous-time event-triggered control

In this subsection, we present an ETC design where the discrete event times at which the control input is updated are determined by continuously evaluating a triggering function similar to the R-CETC scheme in Section 4.1.

Let $I^p = \{t_k^p\}_{k\in\mathbb{N}}$ denote the sequence of event times associated with P-CETC. Let the event-trigger parameters be selected as in Definition 1, and $c > 0$ be an additional design parameter. The P-CETC strategy consists of two parts:

1. An ETC input U_k^p

$$U_k^p := U(t_k^p), \tag{59}$$

for $t \in \left[t_k^p, t_{k+1}^p\right), k \in \mathbb{N}$, where $U(t)$ is given by (9). Then, the boundary condition (8) becomes

$$v(\ell, t) = \rho u(\ell, t) + U_k^p. \tag{60}$$

2. A continuous-time ETM determining event times

$$t_{k+1}^p = \inf\left\{t \in \mathbb{R}_{\geq 0} \mid t > t_k^p, \Gamma^p(t) > 0, k \in \mathbb{N}\right\}, \tag{61}$$

with $t_0^p = 0$. The triggering function $\Gamma^p(t)$ is defined as

$$\Gamma^p(t) := d(t)^2 - \theta m^p(t) - \frac{c}{\theta_m} W^p(t), \tag{62}$$

where $c > 0$ is a free parameter to be selected, $d(t)$ is given by (17), and $m^p(t)$ satisfies the ODE

$$\begin{aligned}\dot{m}^p(t) = &-\eta m^p(t) - \theta_m d(t)^2 + \kappa_{1,1}\|\alpha[t]\|^2 \\ &+ \kappa_{1,2}\|\beta[t]\|^2 + \kappa_{1,3}\alpha(\ell, t)^2 + cW^p(t),\end{aligned} \tag{63}$$

for $t \in \left(t_k^p, t_{k+1}^p\right), k \in \mathbb{N}$ with $m^p\left(t_0^p\right) = m^p(0) > 0$, and $m^p\left(t_k^{p-}\right) = m^p\left(t_k^p\right) = m^p\left(t_k^{p+}\right)$. Here, $W^p(t)$ is the *performance residual*, defined as the difference between the value of the performance-barrier $\mathrm{e}^{-a^\star t}V_0^p$ and the Lyapunov function:

$$W^p(t) := \mathrm{e}^{-a^\star t}V_0^p - V^p(t), \tag{64}$$

where $a^\star$ is given by (49) and $V^p(t)$ is the Lyapunov candidate defined as

$$V^p(t) = V_1(t) + m^p(t), \tag{65}$$

with $V_1(t)$ given by (46) and

$$V_0^p = V^p(0). \tag{66}$$

Remark 5. The only structural difference between the triggering mechanisms used in Espitia (2020), Kang et al. (2023), Lhachemi (2024), Rathnayake and Diagne (2026), Rathnayake, Diagne, Espitia and Karafyllis (2022), Somathilake et al. (2025), Wang and Krstić (2023a) and the P-CETC triggering mechanism is the incorporation of the performance residual $W^p(t)$ in (62). However, the flexibility it provides for adjusting dwell-times is enormous. This improvement can be implemented in the full-state feedback versions of the triggering mechanisms introduced in R-CETC in a modular fashion even without the need to reselect the event-trigger parameters. The ability of the present design to deliver a considerable improvement in dwell-times without adding almost any complexity, while being compatible with already available triggering mechanisms used in works such as Espitia (2020), Kang et al. (2023), Lhachemi (2024), Rathnayake and Diagne (2026), Rathnayake, Diagne, Espitia and Karafyllis (2022), Somathilake et al. (2025), Wang and Krstić (2023a), is powerful.

Next, we state the GEC of the equilibrium of the closed-loop system under P-CETC.

Theorem 4 (*Results under P-CETC*). *Let $I^p = \{t_k^p\}_{k\in\mathbb{N}}$ with $t_0^p = 0$ be the set of event times generated by the P-CETC approach (59)–(66) with appropriate choices for the event-trigger parameters under Definition 1, and $c > 0$. Then, it holds that*

$$\Gamma^p(t) \leq 0, \forall t \in [0, \sup(I^p)). \tag{67}$$

As a result, the following results hold:

- *R1: The set of event times I^p generates an increasing sequence. It holds that $t_{k+1}^p - t_k^p \geq \tau_1 > 0, k \in \mathbb{N}$, where the MDT τ_1 is given by (43). Since $\tau_1 > 0$, as $k \to \infty$, it follows that $t_k^p \to \infty$, thereby guaranteeing Zeno-free behavior.*
- *R2: For every $(u[0], v[0])^T \in L^2\left((0,\ell);\mathbb{R}^2\right)$, there exists a unique solution $(u, v)^T \in C^0\left(\mathbb{R}_+; L^2\left((0,\ell);\mathbb{R}^2\right)\right)$ to the system (5)–(7),(59)–(66) for all $t > 0$.*
- *R3: The dynamic variable $m^p(t)$ governed by (63) with $m^p(0) > 0$ satisfies $m^p(t) > 0$ for all $t > 0$.*
- *R4: The Lyapunov candidate $V^p(t)$ given by (65),(66) satisfies*

$$\dot{V}^p(t) \leq -a^\star V^p(t) + c\left(\mathrm{e}^{-a^\star t}V_0^p - V^p(t)\right), \tag{68}$$

for all $t \in (t_k^p, t_{k+1}^p), j \in \mathbb{N}$, and

$$V^p(t) \leq \mathrm{e}^{-a^\star t}V_0^p, \tag{69}$$

for all $t > 0$, where $a^\star$ is given by (49).

- *R5: The closed-loop signal $\|u[t]\| + \|v[t]\|$ associated with the solution of the system (5)–(7),(59)–(66), exponentially converges to zero. Specifically, the following relationship holds:*

$$\|u[t]\| + \|v[t]\| \leq M_a \mathrm{e}^{-\frac{a^\star}{2}t}\left(\|u[0]\| + \|v[0]\| + \underbrace{m^p(0)^{\frac{1}{2}}}_{GEC}\right),$$

for all $t > 0$ and some constant $M_a > 0$.

Initially, it can be shown that $m^p(t) > 0$ for $t \in [0, \sup\{I^p\})$ using the triggering condition (61),(62) together with the definition of the dynamic variable $m^p(t)$ in (63). Subsequently, one can establish the relation (69) holds; that is, the performance residual satisfies $W^p(t) \geq 0$ for $t \in [0, \sup\{I^p\})$. If R-CETC and P-CETC mechanisms start from the same event time with the same positive dynamic variable states $m^r(t^\star) = m^p(t^\star)$ and the performance residual remains nonnegative until the R-CETC trigger, then it can be shown that the next P-CETC event is no earlier, and hence R1 holds (see Lemma 2 and Theorem 3 of Zhang et al. (2025)). Consequently, results R2, and R3 hold, and properties R4 and R5 are established using the Lyapunov function (65). The proof of Theorem 4 follows reasoning similar to that used in the proof of Theorem 3 in Zhang et al. (2025).

Remark 6. The parameter $c > 0$ in the P-CETC event-trigger (61)–(63) plays a pivotal role in shaping the behavior of the Lyapunov function $V^p(t)$ given by (65). For any c such that $0 < c < \infty$, it follows from R4 of Theorem 4 that $\dot{V}^p(t) \leq -a^\star V^p(t) + c\left(\mathrm{e}^{-a^\star t}V_0^p - V^p(t)\right)$, for all $t \in (t_j^p, t_{j+1}^p), j \in \mathbb{N}$, and consequently, $V^p(t) \leq \mathrm{e}^{-a^\star t}V_0^p$, for all $t > 0$. As described earlier, this allows the Lyapunov function to increase during certain periods as long as it remains below the nominal performance-barrier. As $c \to \infty$, the Lyapunov function approaches the performance-barrier. Conversely, setting $c = 0$ reduces the P-CETC to the R-CETC, resulting in $\dot{V}^p(t) \leq -a^\star V^p(\mathrm{t})$. This demands a strict decrease in the Lyapunov function while ensuring $V^p(t) \leq \mathrm{e}^{-a^\star t}V_0^p$ for all $t > 0$. Fig. 18 in the provided simulations illustrates the behavior of the Lyapunov function for different choices of c. If the performance residual $W^p(t)$ is large — meaning that the Lyapunov function $V^p(t)$ is significantly below the performance barrier $\mathrm{e}^{-a^\star t}V_0^p$ — there is a reduced risk of violating the performance barrier. In such cases, $\dot{V}^p(t)$ can be positive, allowing $V^p(t)$ to increase. Conversely, if $W^p(t)$ is relatively small — meaning the Lyapunov function $V^p(t)$ is approaching the

performance barrier $e^{-a^\star t}V_0^p$ —the risk of breaching the performance barrier increases. In such situations, $\dot{V}^p(t)$ must be negative to ensure that the Lyapunov function remains below the threshold.

In what follows, we introduce a PETC scheme that is obtained by modifying the P-CETC scheme appropriately.

5.2. Performance-barrier periodic event-triggered control

We introduce the P-PETC approach, derived from the P-CETC scheme. This approach is realized by redesigning the triggering function, $\Gamma^p(t)$, of P-CETC to $\tilde{\Gamma}^p(t)$, allowing for periodic evaluation while ensuring that $\Gamma^p(t)$ remains non-positive and the dynamic variable $m^p(t)$ remains positive along the P-PETC closed-loop system solution. Note that the derivation of the P-PETC scheme using the P-CETC framework closely parallels the manner in which the R-PETC scheme is derived.

Let $\tilde{I}^p = \{\tilde{t}_k^p\}_{k\in\mathbb{N}}$ denote the sequence of event times associated with P-PETC, and let the event-trigger parameters $\theta, \theta_m, \kappa_{1,1}, \kappa_{1,2}, \kappa_{1,3} > 0$ be selected as outlined in Definition 1, while η is a parameter to be determined. Note that η is not a free parameter as in Definition 1 under P-PETC. Let $c > 0$ be a free design parameter. The P-PETC strategy consists of two parts:

(1) An ETC input $\tilde{U}_k^p$

$$\tilde{U}_k^p := U(\tilde{t}_k^p), \tag{70}$$

for $t \in \left[\tilde{t}_k^p, \tilde{t}_{k+1}^p\right), k \in \mathbb{N}$, where $U(t)$ is given by (9). Then, the boundary condition (16) becomes

$$v(\ell, t) = \rho u(\ell, t) + \tilde{U}_k^p. \tag{71}$$

(2) A periodic ETM determining the event times

$$\begin{aligned}\tilde{t}_{k+1}^p = \inf\{t \in \mathbb{R}_+ \,|\, t > \tilde{t}_k^p, \tilde{\Gamma}^p(t) > 0, t = nh_1,\\ h_1 > 0, n \in \mathbb{N}, k \in \mathbb{N}\},\end{aligned} \tag{72}$$

with $\tilde{t}_0^p = 0$, h_1 is the sampling period satisfying (53), and the triggering function $\tilde{\Gamma}^p(t)$ defined as

$$\tilde{\Gamma}^p(t) := (a + \theta\theta_m)e^{ah}d(t)^2 - \theta\theta_m d(t)^2 - \theta a m^p(t) - \frac{ac}{\theta_m}e^{-ch}W^p(t), \tag{73}$$

where a is given by (44), $d(t)$ is given by (17) for $t \in \left[\tilde{t}_k^p, \tilde{t}_{k+1}^p\right)$, $k \in \mathbb{N}$, $m^p(t)$ is governed by (63) along the solution of (18)–(21) for $t \in \left(\tilde{t}_k^p, \tilde{t}_{k+1}^p\right), k \in \mathbb{N}$, and $W^p(t)$ is the performance residual given by (64)–(66).

We introduce the following definition for the parameter selection of the subsequent P-PETC and P-STC schemes.

Definition 2. The parameter $\eta > 0$ is selected such that

$$\eta \le \mu - \frac{\max\{\kappa_{1,1}, \kappa_{1,2}\}r}{A}.$$

Therefore, it follows that $\eta = a^\star$ from (49) for the subsequent P-PETC and P-STC designs. While the parameters θ, σ, $\kappa_{1,1}$, $\kappa_{1,2}$, $\kappa_{1,3}$, and θ_m are selected as in Definition 1.

Next, we state the GEC of the equilibrium of the closed-loop system under P-PETC.

Theorem 5 (*Results under P-PETC*). *Let $\tilde{I}^p = \{\tilde{t}_k^p\}_{k\in\mathbb{N}}$ with $\tilde{t}_0^p = 0$ be the set of event times generated by the P-PETC approach (70)–(73) with appropriate choices for the event-trigger parameters under Definition 2, and $c > 0$. Then, the following results hold:*

R1: For every $(u[0], v[0])^T \in L^2((0,\ell);\mathbb{R}^2)$, there exists a unique solution $(u, v)^T \in C^0\left(\mathbb{R}_+; L^2((0,\ell);\mathbb{R}^2)\right)$ to the P-PETC closed-loop system (5)–(7),(70)–(73) for all $t > 0$.

R2: The function $\Gamma^p(t)$ given by (62) satisfies $\Gamma^p(t) \le 0$ for all $t > 0$, along the P-PETC closed-loop solution.

R3: The dynamic variable $m^p(t)$ governed by (63) with $m^p(0) = m^r(0) > 0$ satisfies $m^p(t) > 0$ for all $t > 0$, along the P-PETC closed-loop solution.

R4: The Lyapunov candidate $V^p(t)$ given by (65) satisfies (68) for all $t \in (\tilde{t}_k^p, \tilde{t}_{k+1}^p), k \in \mathbb{N}$ and (69) for all $t > 0$ with $\eta = a^\star$, along the P-PETC closed-loop solution.

R5: The closed-loop signal $\|u[t]\| + \|v[t]\|$ associated with the solution of the system (5)–(7),(70)–(73), exponentially converges to zero. Specifically, the following relationship holds:

$$\|u[t]\| + \|v[t]\| \le M_a e^{-\frac{a^\star}{2}t}\left(\|u[0]\| + \|v[0]\| + \underbrace{m^p(0)^{\frac{1}{2}}}_{GEC}\right),$$

for all $t > 0$ and some constant $M_a > 0$.

Initially, it can be shown that (69) holds given that $\eta = a^\star$ resulting in $W^p(t) \ge 0$ for all $t > 0$. Subsequently, the proof of Theorem 5 follows reasoning similar to that used in the proof of Theorem 2 but, taking the performance residual $W^p(t)$ into account. A detailed proof of Theorem 5 can be found in Zhang et al. (2025).

In what follows, we introduce a STC scheme that is obtained by modifying the P-CETC scheme appropriately.

5.3. Performance-barrier self-triggered control

We introduce the P-STC approach derived from the P-CETC scheme. P-STC determines the next event time at the current event time using prediction of the input holding error detailed in Lemma 2, and by bounding the constituent terms of the P-CETC triggering function $\Gamma^p(t)$. We show the P-STC approach ensures that $\Gamma^p(t)$ given by (62) remains non-positive, and $m^p(t)$ given by (63) remains positive along the P-STC closed-loop system solution. This approach of deriving the P-STC scheme using the P-CETC scheme closely parallels the manner in which the R-STC scheme is derived.

Let $\check{I}^p = \{\check{t}_k^p\}_{k\in\mathbb{N}}$ denote the sequence of event times associated with P-STC, and let the event-trigger parameters $\theta, \theta_m, \kappa_{1,1}, \kappa_{1,2}, \kappa_{1,3}, \eta > 0$ be selected as outlined in Definition 2. Let $c > 0$ be a free design parameter. The P-STC strategy consists of two parts:

1. An event-triggered boundary control input $\check{U}_k^p$

$$\check{U}_k^p := U(\check{t}_k^p), \tag{74}$$

for $t \in \left[\check{t}_k^p, \check{t}_{k+1}^p\right), k \in \mathbb{N}$ where $U(t)$ is given by (9). Then, the boundary condition (8) becomes

$$v(\ell, t) = \rho u(\ell, t) + \check{U}_k^p. \tag{75}$$

2. A self-trigger determining event times

$$\check{t}_{k+1}^p = \check{t}_k^p + G^p\left(F(\check{t}_k^p), m^p\left(\check{t}_k^p\right), W^p(\check{t}_k^p)\right), \tag{76}$$

with $\check{t}_0^p = 0$ and $G^p(\cdot,\cdot,\cdot) > 0$ being a positive function uniformly bounded away from zero satisfying

$$G^p\left(F(t), m^p(t), W^p(t)\right) := \max\left\{\tau_1, \frac{1}{\varrho^\star + \eta + c}\ln\left(\frac{\theta m^p(t) + \frac{\theta\theta_m F(t)}{\varrho^\star + \eta} + \frac{c}{\theta_m}W^p(t)}{F(t) + \frac{\theta\theta_m F(t)}{\varrho^\star + \eta}}\right)\right\}, \tag{77}$$

where τ_1 is the R/P-CETC MDT given by (43). The variable $m^p(t)$ satisfies the dynamics (63) along the solution of (18)–(21) for $t \in \left(\check{t}_k^p, \check{t}_{k+1}^p\right), k \in \mathbb{N}$, $W^p(t)$ is the performance residual given by (64)–(66), and $F(t)$ is given by (28).

Next, we state the GEC of the equilibrium of the closed-loop system under P-STC.

Theorem 6 (*Results under P-STC*). *Let $\check{I}^p = \{\check{t}_k^p\}_{k\in\mathbb{N}}$ with $\check{t}_0^p = 0$ be the set of increasing event times generated by the P-STC approach (74)–(77) with appropriate choices for the event-trigger parameters under Definition 2, and $c > 0$. Then, the following results hold:*

- *R1: For every $(u[0], v[0])^T \in L^2((0,\ell);\mathbb{R}^2)$, there exists a unique solution $(u,v)^T \in C^0(\mathbb{R}_+; L^2((0,\ell);\mathbb{R}^2))$ to the P-STC closed-loop system (5)–(7),(74)–(77) for all $t > 0$.*
- *R2: The function $\Gamma^p(t)$ given by (62) satisfies $\Gamma^p(t) \le 0$ for all $t > 0$, along the P-STC closed-loop solution.*
- *R3: The dynamic variable $m^p(t)$ governed by (63) with $m^p(0) = m^r(0) > 0$ satisfies $m^p(t) > 0$ for all $t > 0$, along the P-STC closed-loop solution.*
- *R4: The Lyapunov candidate $V^p(t)$ given by (65) satisfies (68) for all $t \in (\check{t}_k^p, \check{t}_{k+1}^p), k \in \mathbb{N}$ and (69) for all $t > 0$ with $\eta = a^\star$, along the P-STC closed-loop solution.*
- *R5: The closed-loop signal $\|u[t]\| + \|v[t]\|$ associated with the solution of the system (5)–(7),(74)–(77), exponentially converges to zero. Specifically, the following relationship holds:*

$$\|u[t]\| + \|v[t]\| \le M_a \mathrm{e}^{-\frac{a^\star}{2}t}\left(\|u[0]\| + \|v[0]\| + \underbrace{m^p(0)^{\frac{1}{2}}}_{GEC}\right),$$

for all $t > 0$ and some constant $M_a > 0$.

First, by selecting $\eta = a^\star$, it can be shown that $W^p(t) \ge 0$ for all $t > 0$, similarly to the P-PETC case. Subsequently, by taking the performance residual $W^p(t)$ into account, the proof of Theorem 6 follows reasoning similar to that used in the proof of Theorem 3 (under R-STC). A detailed proof of Theorem 6 is available in Zhang et al. (2025).

This concludes the presentation of the R-ETC scheme and its extension to P-ETC, which allows for longer dwell-times. In the following section, we state a triggering mechanism which yields a stronger stability result.

6. Dynamic switching event-triggered control

In previous sections, only GEC was achieved under the regular ETMs. By introducing a switching dynamic variable, GES can be obtained as shown in Rathnayake and Diagne (2026). In the following developements, we present three switching ETC (S-ETC) schemes: continuous-time event-triggered control (S-CETC), periodic event-triggered control (S-PETC), and self-triggered control (S-STC). The S-ETC schemes presented here are based on the results of Rathnayake and Diagne (2026), with adaptations to the framework considered in this work.

6.1. Switching continuous-time event-triggered control

Following the methodology introduced in Sections 4.1 and 5.1, The S-CETC scheme updates the control input at discrete event times determined by continuous evaluation of an ETM.

Let $I^s = \{t_k^s\}_{k\in\mathbb{N}}$ denote the increasing sequence of event times associated with S-CETC, and it consists of two parts:

1. An ETC input U_k^s

$$U_k^s := U(t_k^s), \tag{78}$$

for $t \in \left[t_k^s, t_{k+1}^s\right), k \in \mathbb{N}$, where $U(t)$ is given by (9). Then, the boundary condition (16) becomes

$$v(\ell,t) = \rho u(\ell,t) + U_k^s. \tag{79}$$

2. A continuous-time ETM determining event times

$$t_{k+1}^s = \inf\left\{t \ge t_k^s + \tau_2 \mid m^s(t) < 0, k \in \mathbb{N}\right\}, \tag{80}$$

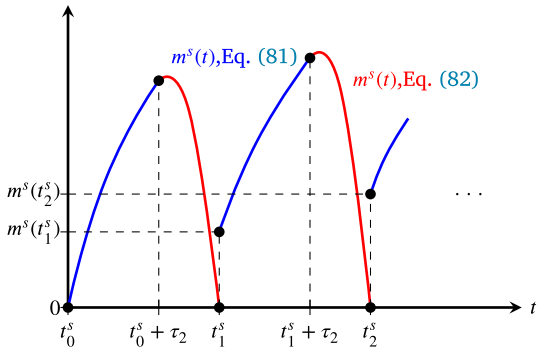

Fig. 13. Schematic of the evolution of the dynamic variable $m^s(t)$ under S-CETC.

with $t_0^s = 0$, where τ_2 is the MDT to be determined and $m^s(t)$ is a dynamic switching variable defined as

$$\begin{aligned}\dot{m}^s(t) = &-\eta m^s(t) + \kappa_{2,1}\|\alpha[t]\|^2 \\ &+ \kappa_{2,2}\|\beta[t]\|^2 + \kappa_{2,3}\alpha(\ell,t)^2,\end{aligned} \tag{81}$$

for all $t \in \left(t_k^s, t_k^s + \tau_2\right), k \in \mathbb{N}$ and

$$\begin{aligned}\dot{m}^s(t) = &-\eta m^s(t) - \theta_n d(t)^2 + \kappa_{2,1}\|\alpha[t]\|^2 \\ &+ \kappa_{2,2}\|\beta[t]\|^2 + \kappa_{2,3}\alpha(\ell,t)^2,\end{aligned} \tag{82}$$

for $t \in \left(t_k^s + \tau_2, t_{k+1}^s\right), k \in \mathbb{N}$ with $m^s\left(t_0^s\right) = m^s(0) = 0$, $m^s(t_k^s) \ge 0, k \in \mathbb{N}$ to be chosen appropriately, and $m^s\left((t_k^s + \tau_2)^-\right) = m^s\left(t_k^s + \tau_2\right), k \in \mathbb{N}$. The parameters $\eta, \theta_n, \kappa_{2,1}, \kappa_{2,2}, \kappa_{2,3} > 0$ are event-trigger parameters to be appropriately chosen.

Under the S-CETC approach, as it can be seen in (81) for $t \in (t_k^s, t_k^s + \tau_2), k \in \mathbb{N}$, $m^s(t)$ remains non-negative. Subsequently, for $t \in (t_k^s + \tau_2, t_{k+1}^s), k \in \mathbb{N}$, since $m^s(t)$ evolves as in (82), where the input holding error $d(t)$ allows $m^s(t)$ to decrease, eventually, the next event occurs according to the triggering condition (80) at time $t = t_{k+1}^s, k \in \mathbb{N}$, which is the zero-crossing of the dynamic variable $m^s(t)$. This evolution of $m^s(t)$ with time t is illustrated in Fig. 13.

Definition 3. The parameters $\eta, \kappa_{2,1}, \kappa_{2,2}, \kappa_{2,3} > 0$ are free parameters to be selected, and θ_n is selected as

$$\theta_n = b_2\omega_0^2 + b_1\omega_0 + b_0, \tag{83}$$

where $b_1, b_2, \omega_0 > 0$, and

$$b_0 = 2Bq^2\mathrm{e}^{\mu\frac{\ell}{\lambda_2}} + \frac{\varepsilon_0}{b_2}. \tag{84}$$

The constant B is selected as

$$\begin{aligned}B > \max\Bigg\{ &\frac{\mathrm{e}^{\mu\frac{\ell}{\lambda_1}}}{1 - 2\rho^2 q^2 \mathrm{e}^{\mu\left(\frac{\ell}{\lambda_1}+\frac{\ell}{\lambda_2}\right)}}\left(\frac{\varepsilon_3}{b_2} + \kappa_{2,3}\right), \\ &\frac{r}{\mu}\max\left\{\frac{\varepsilon_1}{b_2} + \kappa_{2,1}, \frac{\varepsilon_2}{b_2} + \kappa_{2,2}\right\}\Bigg\},\end{aligned} \tag{85}$$

with r and μ defined in (39) and (41), respectively. Consider the following piecewise right continuous reset function $f(t) : \mathbb{R}_{\ge 0} \to \mathbb{R}_{>0}$:

$$\dot{f}(t) := \begin{cases} -b_2 f(t)^2 - b_1 f(t) - b_0, & \forall t \in (t_k^s, t_k^s + \tau_2), \\ 0, & \forall t \in (t_k^s + \tau_2, t_{k+1}^s), \end{cases} \tag{86}$$

for $k \in \mathbb{N}$, where $f(t_k^s) = \omega_1 > 0$, $f((t_k^s + \tau_2)^-) = f(t_k^s + \tau_2) = f((t_k^s + \tau_2)^+)$ and τ_2 is the MDT given by

$$\tau_2 = \int_{\omega_0}^{\omega_1} \frac{1}{b_2 s^2 + b_1 s + b_0} ds, \tag{87}$$

where ω_1 is selected such that $\omega_1 > \omega_0$. Refer to Rathnayake and Diagne (2026) for an explicit expression of the MDT, τ_2 in (87).

Further, select the initial conditions of $m^s(t)$ satisfying (81),(82) as

$$m^s(t_0^s) = m^s(0) = 0, \tag{88}$$

$$m^s((t_k^s + \tau_2)^-) = m^s(t_k^s + \tau_2), k \in \mathbb{N}, \tag{89}$$

$$m^s(t_k^s) = \omega_0 d((t_k^s)^-)^2 = \omega_0 (U_k^s - U_{k-1}^s)^2, k \in \mathbb{N}_{>0}. \tag{90}$$

Next, we state the GES of the equilibrium of the closed-loop system under S-CETC.

Theorem 7 (*Results under S-CETC*). *Let $I^s = \{t_k^s\}_{k\in\mathbb{N}}$ with $t_0^s = 0$ be the set of event times generated by the S-CETC approach (78)–(82) with appropriate choices for the event-trigger parameters under Definition 3. Then it holds that*

R1: The set of event times I^s generates an increasing sequence. It holds that $t_{k+1}^s - t_k^s \geq \tau_2 > 0, k \in \mathbb{N}$, where τ_2 is given by (87). Due to the existence of a uniform positive MDT $\tau_2 > 0$, it follows that $t_k^s \to \infty$ as $k \to \infty$, thereby guaranteeing Zeno-free behavior.

R2: For every $(u[0], v[0])^T \in L^2\left((0,\ell);\mathbb{R}^2\right)$, there exists a unique solution $(u, v)^T \in C^0\left(\mathbb{R}_+; L^2\left((0,\ell);\mathbb{R}^2\right)\right)$ to the system (5)–(7),(78)–(82) for all $t > 0$.

R3: The dynamic variable $m^s(t)$ governed by (81),(82),(88)–(90) satisfies $m^s(t) \geq 0$ for all $t > 0$, along the S-CETC closed-loop solution.

R4: Consider a Lyapunov candidate

$$V^s(t) = V_2(t) + f(t)d(t)^2 + m^s(t), \tag{91}$$

where

$$V_2(t) := \int_0^\ell \left(\frac{B}{\lambda_1}\alpha^2(x,t)\mathrm{e}^{-\mu\frac{x}{\lambda_1}} + \frac{Bq^2}{\lambda_2}\beta^2(x,t)\mathrm{e}^{\mu\frac{x}{\lambda_2}}\right)dx. \tag{92}$$

Then it holds that

$$\dot{V}^s(t) \leq -b^\star V^s(t), \tag{93}$$

for all $t \in (t_k^s, t_k^s + \tau_2) \cup (t_k^s + \tau_2, t_{k+1}^s), k \in \mathbb{N}$, and

$$V^s(t) \leq \mathrm{e}^{-b^\star t} V^s(0), \tag{94}$$

for all $t > 0$, where

$$b^\star := \min\left\{\mu - \frac{r}{B}\max\left\{\frac{\varepsilon_1}{b_2} + \kappa_{2,1}, \frac{\varepsilon_2}{b_2} + \kappa_{2,2}\right\}, b_1, \eta\right\} > 0. \tag{95}$$

See Definition 3 for details on $\mu, \kappa_{2,1}, \kappa_{2,2}, r, B, \eta > 0$.

R5: The closed-loop signal $\|u[t]\| + \|v[t]\|$ associated with the solution of the system (5)–(7), (78)–(82), exponentially stabilizes to zero. Specifically, the following relationship holds:

$$\|u[t]\| + \|v[t]\| \leq M_b \mathrm{e}^{-\frac{b^\star}{2}t}\left(\|u[0]\| + \|v[0]\|\right),$$

for all $t > 0$ and some constant $M_b > 0$.

By virtue of (81), $m^s(t)$ is guaranteed to remain non-negative for $t \in (t_k^s, t_k^s + \tau_2), k \in \mathbb{N}$, thereby establishing the existence of a MDT under the ETM (80)–(82), consequently resulting in R1 of the above theorem. Consequently, result R2 is achieved using Proposition 1. Result R3 is a direct outcome of the definition of $m^s(t)$ in (81),(82) and the triggering condition (80). Finally, utilizing R2,R3, and the Lyapunov function candidate (91), the results R4 and R5 can be obtained. The proof of the above theorem follows directly from the results in Rathnayake and Diagne (2026).

Remark 7. Unlike the R-ETC and P-ETC methods in Sections 4 and 5, respectively, in which the dynamic variables $m^r(t)$ and $m^p(t)$ evolve continuously between events, the switching dynamics considered here permit the initial condition of the dynamic variable to be defined as $m^s(0) = 0$. This change in the definition of the dynamic variable allows for the GES of the spatial L^2 norm (R5 of Theorem 7) under S-ETC as opposed to GEC of the spatial L^2 norm under R-ETC and P-ETC.

In what follows, we introduce a PETC scheme that preserves the stability guarantees established for S-CETC.

6.2. Switching periodic event-triggered control

The S-PETC is conceived by constructing a new dynamic variable $\tilde{m}^s(t)$ that is evaluated periodically while still ensuring that $m^s(t)$ remains non-negative along the closed-loop system trajectory. Let $\tilde{I}^s = \{\tilde{t}_k^s\}_{k\in\mathbb{N}}$ denote the increasing sequence of event times associated with S-PETC, and it consists of two parts:

1. An ETC input $\tilde{U}_k^s$

$$\tilde{U}_k^s := U(\tilde{t}_k^s), \tag{96}$$

for $t \in \left[\tilde{t}_k^s, \tilde{t}_{k+1}^s\right), k \in \mathbb{N}$, where $U(t)$ is given by (9). Then, the boundary condition (16) becomes

$$v(\ell, t) = \rho u(\ell, t) + \tilde{U}_k^s. \tag{97}$$

2. A periodic ETM determining event times

$$\tilde{t}_{k+1}^s = \inf\left\{t \geq \tilde{t}_k^s + \tau_2 \mid \tilde{m}^s(t) < 0, t = nh_2, n \in \mathbb{N}, k \in \mathbb{N}\right\}, \tag{98}$$

with $\tilde{t}_0^s = 0$, where τ_2 is the MDT to be determined and

$$\tilde{m}^s(t) = m^s(t) - \frac{\theta_n}{a}(\mathrm{e}^{ah_2} - 1)d(t)^2, \tag{99}$$

where $m^s(t)$ satisfies (81),(82). The sampling period, h_2 is the selected such that

$$0 < h_2 \leq \min\left\{\tau_2, \frac{1}{a}\ln\left(1 + \frac{\kappa_{2,1}a}{\varepsilon_1\theta_n}\right), \frac{1}{a}\ln\left(1 + \frac{\kappa_{2,2}a}{\varepsilon_2\theta_n}\right), \frac{1}{a}\ln\left(1 + \frac{\kappa_{2,3}a}{\varepsilon_3\theta_n}\right)\right\}, \tag{100}$$

and $\frac{\tau_2}{h_2} \in \mathbb{N}_{>0}$ for any $\kappa_{2,1}, \kappa_{2,2}, \kappa_{2,3} > 0$, ε_1, ε_2, ε_3 as defined in (24)–(26), and a, θ_n, as defined in (44), (83) respectively.

Next, we state the GES of the equilibrium of the closed-loop system under S-PETC.

Theorem 8 (*Results under S-PETC*). *Let $\tilde{I}^s = \{\tilde{t}_k^s\}_{k\in\mathbb{N}}$ with $\tilde{t}_0^s = 0$ be the set of event times generated by the S-PETC approach (96)–(100) with appropriate choices for the event-trigger parameters under Definition 3. Then it holds that*

R1: For every $(u[0], v[0])^T \in L^2\left((0,\ell);\mathbb{R}^2\right)$, there exists a unique solution $(u, v)^T \in C^0\left(\mathbb{R}_+; L^2\left((0,\ell);\mathbb{R}^2\right)\right)$ to the system (5)–(7),(96)–(100) for all $t > 0$.

R2: The dynamic variable $m^s(t)$ governed by (81),(82),(88)–(90) satisfies $m^s(t) \geq 0$ for all $t > 0$, along the S-PETC closed-loop solution.

R3: The Lyapunov candidate $V^s(t)$ given by (91),(92) satisfies (93) for all $t \in (\tilde{t}_k^s, \tilde{t}_k^s + \tau_2) \cup (\tilde{t}_k^s + \tau_2, \tilde{t}_{k+1}^s), k \in \mathbb{N}$, and (94) for all $t > 0$, along the S-PETC closed-loop solution.

R4: The closed-loop signal $\|u[t]\| + \|v[t]\|$ associated with the solution of the system (5)–(7), (96)–(99), exponentially stabilizes to zero. Specifically, the following relationship holds:

$$\|u[t]\| + \|v[t]\| \leq M_b \mathrm{e}^{-\frac{b^\star}{2}t}\left(\|u[0]\| + \|v[0]\|\right),$$

for all $t > 0$ and some constant $M_b > 0$.

Since the triggering function is evaluated periodically under S-PETC, Zeno phenomenon is inherently excluded and the set of event times $\tilde{I}^s$ generates an increasing sequence. Subsequently, using Proposition

1, result R1 can be established. Note that $m^s(t) \geq 0$ for any $t \in [\tilde{t}_k^s, \tilde{t}_k^s + \tau_2), k \in \mathbb{N}$. Given that the sampling period h_2 is selected to satisfy (100), $\tilde{m}^s(t)$ in (99) is defined such that if $\tilde{m}^s(nh_2) \geq 0$ for any $n \in [(\tilde{t}_k^s + \tau_2)/h_2, \tilde{t}_{k+1}^s/h_2) \cap \mathbb{N}, k \in \mathbb{N}$, $m^s(t) \geq 0$ for all $t \in [nh_2, (n+1)h_2)$. Therefore, even though the triggering condtion is evaluated only at periodic sampling instants, as specified in (98), $m^s(t) \geq 0$ for $t \in [\tilde{t}_k^s, \tilde{t}_{k+1}^s), k \in \mathbb{N}$. Since the triggering condition (80)–(82) is satisfied for all $t > 0$ and the results in Theorem 7 holds under S-PETC. The proof of the above theorem follows directly from the results in Rathnayake and Diagne (2026).

In what follows, we introduce a STC scheme that preserves the stability guarantees established for S-CETC.

6.3. Switching self-triggered control

The S-STC approach allows for the determination of the next event time from information available at the current event time by utilizing the estimate of the input holding error in Lemma 2 while bounding $m^s(t)$ appropriately to ensure its non-negativity along the closed-loop system trajectory. Most importantly, compared to the previously introduced ETMs that ensure GEC and GES, the S-STC scheme does not require continuous monitoring of the PDE state and relies solely on sampled information at current and prior events.

Let $\check{I}^s = \{\check{t}_k^s\}_{k\in\mathbb{N}}$ denote the increasing sequence of event times associated with S-STC, and it consists of two parts:

1. An ETC input $\check{U}_k^s$

$$\check{U}_k^s := U(\check{t}_k^s), \tag{101}$$

for $t \in \left[\check{t}_k^s, \check{t}_{k+1}^s\right), k \in \mathbb{N}$, where $U(t)$ is given by (9). Then, the boundary condition (16) becomes

$$v(\ell, t) = \rho u(\ell, t) + \check{U}_k^s. \tag{102}$$

2. A self-triggered trigger condition

$$\check{t}_1^s = \check{t}_0^s + \tau_2, \tag{103}$$

$$\check{t}_{k+1}^s = \check{t}_k^s + \tau_2 + \frac{1}{\varrho^\star + \eta} \times \ln\left(1 + \frac{(\varrho^\star + \eta)\omega_0(\check{U}_k^s - \check{U}_{k-1}^s)^2}{\theta_n e^{(\varrho^\star+\eta)\tau_2}(F(\check{t}_k^s) + \epsilon)}\right), \tag{104}$$

for $k \in \mathbb{N}_{>0}$, and $\omega_0, \eta, \epsilon > 0$ are free parameters to be selected with $F(t)$, τ_2, $\varrho^\star$ defined in (28), (87), (30) respectively.

Next, we state the GES of the equilibrium of the closed-loop system under S-STC.

Theorem 9 (*Results under S-STC*). *Let $\check{I}^s = \{\check{t}_k^s\}_{k\in\mathbb{N}}$ with $\check{t}_0^s = 0$ be the set of event times generated by the S-STC approach (101)–(104) with appropriate choices for the event-trigger parameters under Definition 3. Then it holds that*

- *R1: For every $(u[0], v[0])^T \in L^2\left((0,\ell);\mathbb{R}^2\right)$, there exists a unique solution $(u, v)^T \in C^0\left(\mathbb{R}_+; L^2\left((0,\ell);\mathbb{R}^2\right)\right)$ to the system (5)–(7),(101)–(104) for all $t > 0$.*
- *R2: The dynamic variable $m^s(t)$ governed by (81),(82),(88)–(90) satisfies $m^s(t) \geq 0$ for all $t > 0$, along the S-STC closed-loop solution.*
- *R3: The Lyapunov candidate $V^s(t)$ given by (91),(92) satisfies (93) for all $t \in (\check{t}_k^s, \check{t}_k^s + \tau_2) \cup (\check{t}_k^s + \tau_2, \check{t}_{k+1}^s), k \in \mathbb{N}$, and (94) for all $t > 0$, along the S-STC closed-loop solution.*
- *R4: The closed-loop signal $\|u[t]\| + \|v[t]\|$ associated with the solution of the system (5)–(7), (101)–(104), exponentially stabilizes to zero. Specifically, the following relationship holds:*

$$\|u[t]\| + \|v[t]\| \leq M_b e^{-\frac{b^\star}{2}t}\left(\|u[0]\| + \|v[0]\|\right),$$

for all $t > 0$ and some constant $M_b > 0$.

The set of event times $\check{I}^s$ generates an increasing sequence as the triggering condition (103),(104) is defined such that the Zeno phenomenon is excluded. Hence, using Proposition 1, result R1 can be shown. Now, under the ETM defined by (103),(104) along with Lemma 2, it can be shown that R2 holds. Subsequently, R3 and R4 follow since the triggering condition (80)–(82) is satisfied for all $t > 0$ and the results in Theorem 7 hold under S-STC. The proof of the above theorem can be found in Rathnayake and Diagne (2026).

Following the discussion of the various ETMs, numerical simulations are provided to validate the theoretical results developed above.

7. Numerical simulations

We consider the Saint-Venant Eqs. (1),(2) with the boundary conditions (3),(4), where the parameters are set as $\ell = 10$ m, $g = 9.81\ \mathrm{m\,s^{-2}}$, $C_f = 0.2$, $k_G = 0.6$, $Q_0 = 2\ \mathrm{m^3\,s^{-1}}$, and $H_G = 0.1$ m. The desired water height and water velocity at equilibrium are chosen as $H_{eq} = 2$ m and $V_{eq} = 1\ \mathrm{m\,s^{-1}}$, such that Assumption 2 and the boundary condition (3) are satisfied. The channel bottom slope is selected as $S_b = C_f V_{eq}^2/(gH_{eq}) \approx 0.01019$, ensuring that Assumption 1 holds. The proposed control designs are evaluated on the linearized system (5)–(7),(16). The initial conditions are set as $H(x,0) = 2 - \sin\left(\frac{\pi}{\ell}x\right)$ m and $V(x,0) = 1 + \frac{1}{2}\sin\left(\frac{3\pi}{\ell}x\right)\ \mathrm{m\,s^{-1}}$.

The parameter selection for the triggering mechanisms is as follows. The constants $\varepsilon_0, \varepsilon_1, \varepsilon_2$, and ε_3 are determined from (23)–(26), while $\bar{\mu}$, $\varrho^\star$, and ϱ are determined from (29)–(31). The following free positive design parameters are specified as follows: $\theta = 5$, $\sigma = 0.5$, $b_2 = 1$, $\omega_0 = 5$, $\omega_1 = 250$, $\kappa_{2,1} = 1$, $\kappa_{2,2} = 1$, $\kappa_{2,3} = 1$, $\epsilon = 1\times10^{-11}$ and $c = 1\times10^{-4}$. The parameters $\kappa_{1,1}$, $\kappa_{1,2}$, $\kappa_{1,3}$ are determined from (37), and $\mu = 0.016$ is selected to satisfy (39). The constants A, B are selected as $A = 12.4026$ and $B = 2428.04$, ensuring the inequalities (40),(85) hold. By selecting $\eta = 0.0106$, the relationship $a^\star = \eta$ is satisfied. Note that η is a free design parameter for all the triggering mechanisms except P-PETC and P-STC, and is chosen uniformly for simplicity. Consequently, θ_m can be determined from (38). With a as defined in (44), the MDT under R-ETC and P-ETC, τ_1 is calculated from (43) as $\tau_1 = 0.0187$ s and the sampling interval under R-PETC and P-PETC is chosen as $h_1 = 0.0185$ s. Additionally, b_0 is determined from (84) and the free design parameter b_1 is selected as $b_1 = 2\sqrt{b_0 b_2}$ which allows θ_n to be computed from (83). Using these constants, the MDT under S-ETC, τ_2 is calculated as $\tau_2 = 0.0165$ s, and the sampling interval under S-PETC is determined from (100) as $h_2 = 0.0165$ s.

The PDEs (5)–(7), (16) are solved using an explicit finite difference scheme with a time step $\Delta t = 5 \times 10^{-4}$ s and a spatial step $\Delta x = 0.05$ m, satisfying the Courant–Friedrichs–Lewy (CFL) condition under the transport speeds $\lambda_1 = 5.4294\ \mathrm{m\,s^{-1}}$ and $\lambda_2 = 3.4294\ \mathrm{m\,s^{-1}}$. The simulation was run for 500 s.

Figs. 14, 15, and 16 show the evolution of the spatial L^2 norm of the characteristic coordinates, the control input, and the dwell-times under each triggering condition, respectively. It should be noted that the P-ETC scheme, designed to allow larger dwell-times, results in slower convergence of the spatial L^2 norm to zero. Consequently, the results under P-ETC in Figs. 14(b),15(b),16(b) are shown over 500 s. In contrast, under R-ETC and S-ETC, the L^2 norm of the characteristic coordinates converges to zero significantly faster, and thus the corresponding results are presented over 70 s.

Note that from Figs. 14, 15, the systems exhibit similar performance under CETC and PETC schemes. In contrast, under STC, which is the most conservative of the triggering conditions, control input updates occur more frequently, resulting in the fastest convergence of the spatial L^2 norm of the characteristic coordinates to zero. The conservative nature of STC is further evident in Fig. 16 where the dwell-times under STC are much shorter than those under CETC and PETC. In particular, as shown in Fig. 16(c), S-STC is the most conservative of all the triggering conditions presented. Under S-STC, the dwell-time is always

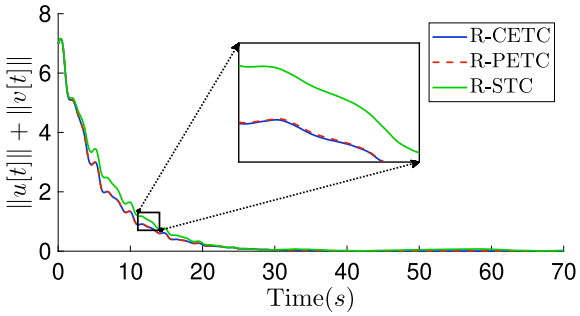

(a) Evolution of the spatial L^2 norm of the characteristics under R-ETC.

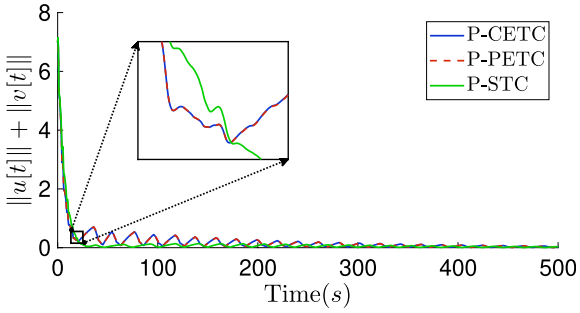

(b) Evolution of the spatial L^2 norm of the characteristics under P-ETC.

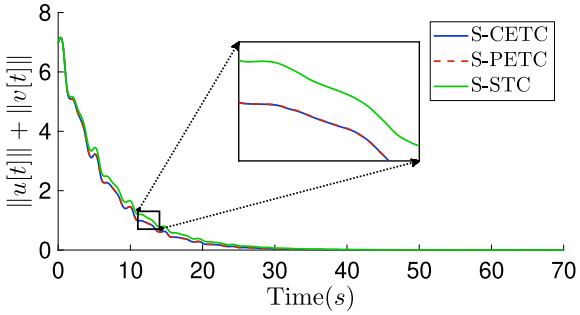

(c) Evolution of the spatial L^2 norm of the characteristics under S-ETC.

Fig. 14. Evolution of the spatial L^2 norm of the characteristics under the ETC schemes.

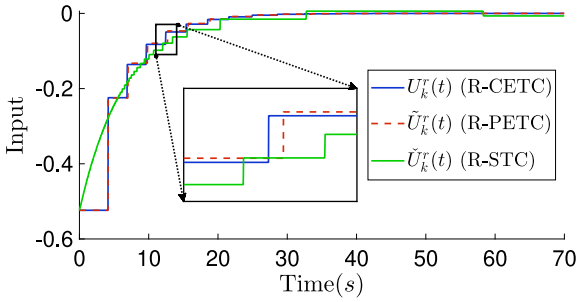

(a) Evolution of the control input under R-ETC.

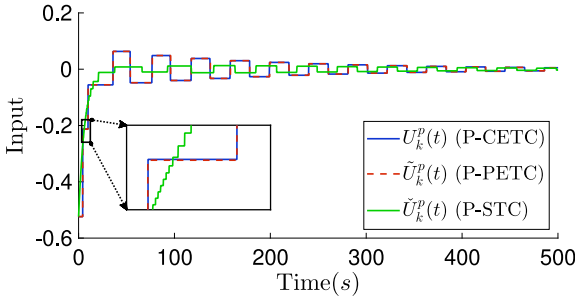

(b) Evolution of the control input under P-ETC.

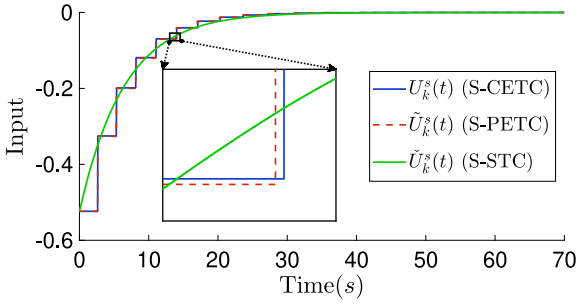

(c) Evolution of the control input under S-ETC.

Fig. 15. Evolution of the control input under the ETC schemes.

at least equal to the MDT τ_2. It was observed that $\check{t}_{k+1}^s - \check{t}_k^s - \tau_2 \leq \Delta t, k \in \mathbb{N}$ for most events, resulting in an average dwell-time close to τ_2. Although this is undesirable, all of the methods considered still offer a significant advantage over implementing the CTC design, where the control input must be updated at every simulation step.

Selection of the free design parameters. A key advantage of implementing dynamic triggering conditions is the additional design flexibility provided by the free design parameters. In particular, for S-STC, where the shortest dwell-times were observed, dedicated tuning of these parameters can yield significantly larger inter-event times. Consider S-STC design with $\kappa_{2,1} = \kappa_{2,2} = \kappa_{2,3} = 10^{-10}$, $b_2 = 0.003$, $b_1 = 2\sqrt{b_0 b_2}$, $\omega_0 = 500$, $\omega_1 = 25000$, and $\eta = 10^{-10}$. These parameters yield an MDT of $\tau_2 = 2.001$ s. The spatial L^2 norm, control input, and the dwell-times under S-STC with these design parameters are shown in Fig. 17. The dwell-times exhibit only small deviations from the MDT, with an average dwell-time of 2.003 s. This limited deviation may be attributed to the system dynamics and the conservative nature of the control design. Nevertheless, the tuning of the triggering parameters enables substantially larger inter-event times by increasing the MDT.

In addition, to illustrate the influence of the parameter c on the performance of P-ETC scheme, Fig. 18 shows the evolution of the Lyapunov function $V^p(t)$ in (65) under P-CETC for different values of $c > 0$. As c increases, $V^p(t)$ is allowed to approach the barrier $V_0^p \mathrm{e}^{-a^\star t}$ more closely, while still satisfying (69) by having greater dwell-times. To further show the effect of the value of c on the dwell-times Table 1 shows the average dwell-time over the span of 500 s under each triggering condition and for different values of c under P-ETC.

8. Concluding remarks and perspectives

In this review article, we presented several ETMs that allow reduction of the cost of actuation of PDE systems using backstepping designs. Our frameworks can be viewed as a step towards the digitization of continuous-time PDE backstepping controllers via CETC, PETC and STC. Our regular designs R-PETC and R-STC extend the dynamic R-CETC proposed in the literature, while our performance barrier designs sparsify the event triggering to further diminish the actuation cost. The aforementioned schemes allow for GEC while our switching dynamic ETMs allow for GES. The Saint-Venant equations of shallow water wave has been used as a benchmark model that embodies the concepts presented in this review and exhaustive simulation results are conducted to illustrate the feasibility of our designs. Below, we suggest a few open problems that could expand further the development of ETC for PDE systems.

Table 1
Average dwell-times (Avg. DTs) in seconds over a period of 500 s. R-ETC is a special case of P-ETC with $c = 0$ whereas S-ETC is a triggering mechanism separate from both R-ETC and P-ETC.

	R-ETC	P-ETC					S-ETC
	$c = 0$	$c = 0.0001$	$c = 0.001$	$c = 0.01$	$c = 0.1$	$c = 1$	–
CETC Avg. DTs [s]	5.95	18.68	18.68	21.46	19.64	19.81	7.68
PETC Avg. DTs [s]	7.05	18.69	18.69	21.37	19.64	19.81	6.02
STC Avg. DTs [s]	3.14	3.39	3.39	3.63	5.55	7.24	0.02

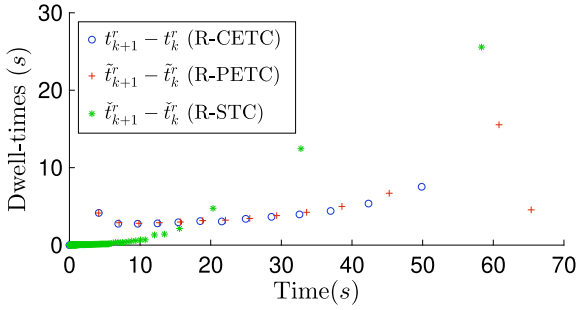

(a) Dwell-times under R-ETC.

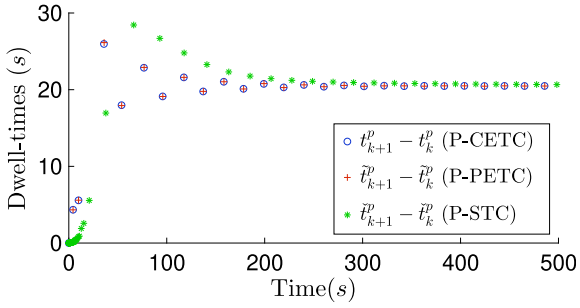

(b) Dwell-times under P-ETC.

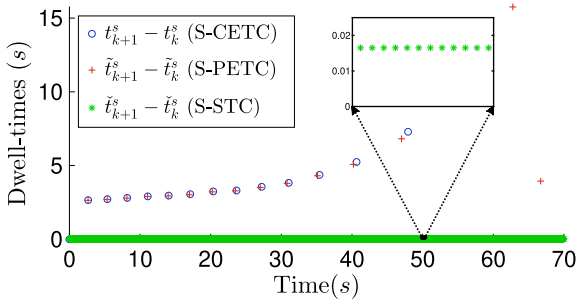

(c) Dwell-times under S-ETC.

Fig. 16. Dwell times under the ETC schemes.

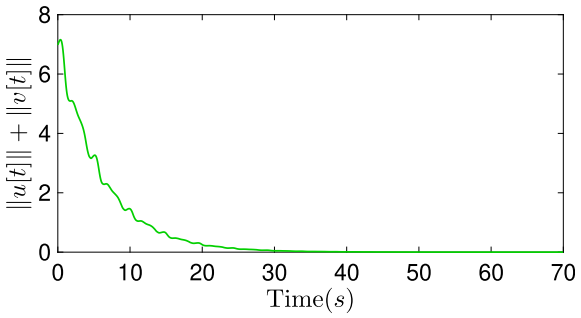

(a) Evolution of the spatial L^2 norm of the characteristics under S-STC.

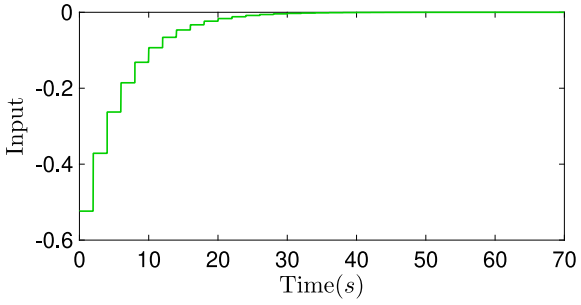

(b) Evolution of the control input under S-STC.

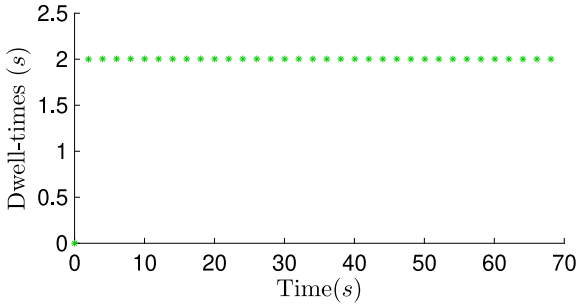

(c) Dwell-times under S-STC.

Fig. 17. System performance for S-STC under modified design parameters.

Extension to more complex classes of systems or control objective. The regular and switching CETC, PETC, and STC frameworks outlined in this review article open several promising research avenues. A natural next step is to extend our PETC, STC, S-CETC, S-PETC and S-STC designs to more complex PDE-ODE coupled systems, including string-actuated processes and structured PDE-PDE cascades, as considered in Wang and Krstić (2022a, 2022b, 2022c). The ETMs in the aforementioned contributions , developed using the methodology summarized in Section 4, provide global exponential *convergence* to an equilibrium set, rather than global exponential *stability*, which can be achieved with the help of the ETMs presented in Section 6. In summary, our developments allow for the design of periodic and self-triggered boundary controllers to guarantee stronger stability properties for broader classes of cascade and coupled systems. For example,

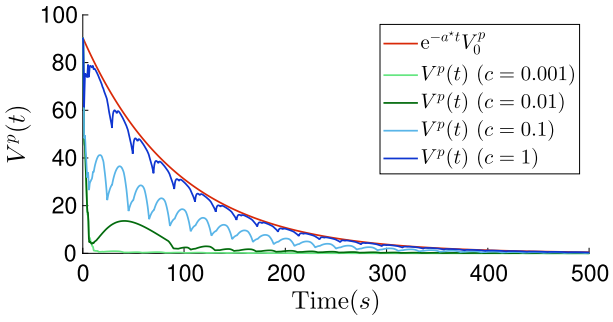

Fig. 18. Behavior of the Lyapunov function $V^p(t)$ under different choices of c under P-CETC.

in the context of sandwiched hyperbolic PDEs motivated by mining-cable applications, CETC-based designs can yield highly conservative lower bounds on the dwell-time (e.g., $\tau = 0.15\times10^{-9}$). Combining P-ETC and S-ETC could alleviate this limitation by yielding sparser triggering instants while enabling S-PETC and S-STC designs that ensure GES; the same observation applies to Wang and Krstić (2022a, 2022b, 2022c). A theoretical development that is left open but tractable is the construction of an observer-based performance barrier design that has not been realized for ODEs (Ong & Cortés, 2024) and PDE (Rathnayake et al., 2024; Zhang et al., 2025) systems where the measurements of the full state is required.

Event-triggered adaptive and learning control. The algorithms presented in this review article do not account for uncertainties on plant parameters, which could be integrated into both regular PETC and STC as well as switching ETC, PETC and STC following Wang and Krstić (2023a, 2023b). The designs are compatible with adaptive control designs based on Lyapunov design, swapping design, passive identifiers (Smyshlyaev & Krstić, 2010) or batch least-squares identifiers (Karafyllis et al., 2020). The recent contributions on Deep learning of PDE backstepping gain kernels via DeepONet (Bhan et al., 2024; Wang, Diagne, & Krstić, 2025a, 2025b) apply to ETC designs as shown in our contribution (Yuan et al., 2025), which can be further advanced to adaptive ETC via DeepONet following Lamarque et al. (2025).

Concurrent event-triggered and gain-scheduled control. To avoid conflation, we first recall the notion of *co-design* in the context of ETC. As stated in Section 1, ETC can be derived either by emulation or by co-design. In the emulation approach, a pre-designed stabilizing CTC signal is sampled at the event times to update the control input. In contrast, the co-design ETC (Co-ETC) approach entails the joint design of both the piecewise-constant control law and the ETM. For instance, Co-ETC design for the boundary control of nonlinear infinite-dimensional plants, such as highly re-entrant manufacturing systems, have been explored in Diagne and Karafyllis (2021). Here, by concurrent event-triggered and gain-scheduled control (Co-ETGSC), we refer to a control design in which concurrent sampling of a time-varying controller gain (gain scheduling) and the system state (state sampling), where both the gain scheduler and the state-triggering mechanism are simultaneously executed. This remains distinct from Co-ETC since Co-ETGSC can be based on either co-design or emulation. For nonlinear ODE systems, Co-ETGSC methods have been studied in finite-dimensional settings (Coutinho & Palhares, 2022). However, for PDE systems with time-dependent parameters (Coron et al., 2021) (see Anfinsen and Aamo (2018), Deutschmann et al. (2016) for a single hyperbolic PDE), the resulting gain kernel PDE is also time-dependent, which makes their real-time computation extremely challenging. Reducing the computational burden has been performed in Espitia and Auriol (2025), Karafyllis et al. (2021) for RD PDEs with spatially and temporally varying reactivity and 2×2 hyperbolic PDEs with time- and space-dependent coupling coefficients. An interesting future direction is to develop a Co-ETGSC for PDE systems. Such a extension is far from trivial because the input holding error induced by the simultaneous sampling of the gain and the state might not result in a system whose Lyapunov stability and existence of MDT are easy to prove by combining the approach in Espitia and Auriol (2025) and Espitia et al. (2016, 2021). The development of Co-ETGSC may apply to PETC and STC while a sparsification of the event-triggers could result from our P-ETC scheme. Furthermore, the design of an observer-based Co-ETGSC remains an open problem given that the results in Espitia and Auriol (2025), Karafyllis et al. (2021) require full-state measurements.

Event-triggered estimation. For PDE control based on the emulation of PDE backstepping controller, the focus has primarily been on designing ETMs for actuators until the recent result (Zhao & Vazquez, 2026) proposing a dynamic ETM that achieves GEC by triggering the sensor of a 2×2 hyperbolic system with boundary disturbance. The result of Zhao and Vazquez (2026) can be extended to R-PETC, R-STC, P-ETC, P-PETC and P-STC designs following the results presented in Sections 4 and 5. Furthermore, a stronger result that pertains to achieving GES exploiting the switching dynamic ETMs introduced in Section 6 is an interesting research topic.

Further research perspectives. The development of ETC of PDEs has been limited to 2×2 hyperbolic systems and scalar RD PDEs because the proof of well-posedness for higher-order systems is not evident. Note that for n coupled RD PDEs (Vazquez & Krstić, 2017), the well-posedness of the resulting closed-loop system under continuous-time backstepping controller has only been assumed rather than established. Extending the ETMs to higher-order systems such as general coupled RD and hyperbolic systems remains an open and challenging research problem that requires further investigation. Particularly, the extension to $n+1$ or $n+m$ hyperbolic systems (Di Meglio et al., 2013; Hu et al., 2016) could lead to the ETC of networks of open-channel flows, which is a practically relevant problem to water distribution systems or fluvial networks (de Halleux et al., 2003). Nevertheless, extending emulation-based ETC methods to these higher-order PDEs remains challenging due to the complexity of the underlying continuous-time design and the well-posedness issues induced by a piecewise-constant boundary control input. Additionally, higher-dimensional systems—such as 3-D reaction–advection–diffusion PDEs for leader–follower multi-agent deployment (Qi et al., 2015, 2019; Wang et al., 2024) have not been addressed in the current literature as well as output-feedback tracking control or disturbance rejection by emulation of the design presented in Anfinsen and Aamo (2015, 2020). Practically, the linearized Saint-Venant model can possibly be exposed to nonlinear disturbances arising from significant fluctuations in the water level and flow velocity, which raises the question of robustness of ETC for PDE systems. We note that adaptive ETC of coupled linear hyperbolic PDEs, building upon the R-ETC framework presented in this work, has also been investigated in Wang et al. (2021) for the case where the constant plant parameters are unknown. However, few studies have been dedicated to event-based design subject to in-domain or boundary disturbances (Zhao & Vazquez, 2026). Furthermore, in practical water-management and irrigation systems, communication between remotely located sluice gates and sensors often relies on wireless networks, which can introduce communication delays. This naturally motivates extending the present framework to account for actuator and/or sensor dynamics. Delayed actuation or sensing can be modeled by an advection PDE governing the actuator or sensor dynamics (Krstić & Bekiaris-Liberis, 2013), resulting in a boundary control problem for a hyperbolic PDE–PDE cascade. For RD PDEs, compensation of boundary input delays via ETC has recently been achieved, resulting in a cascade of a hyperbolic PDE and a parabolic PDE (Koudohode et al., 2024) and the R-ETC framework presented in Section 4 can be extended similarly for hyperbolic systems with delays.

Declaration of competing interest

The authors declare that they have no known competing financial interests or personal relationships that could have appeared to influence the work reported in this paper.

Data availability

No data was used for the research described in the article.

References

Abdelrahim, Mahmoud, Postoyan, Romain, Daafouz, Jamal, & Nešić, Dragan (2016). Stabilization of nonlinear systems using event-triggered output feedback controllers. *IEEE Transactions on Automatic Control*, *61*(9), 2682–2687.

Ahmed-Ali, Tarek, Karafyllis, Iasson, Giri, Fouad, Krstić, Miroslav, & Lamnabhi-Lagarrigue, Francoise (2017). Exponential stability analysis of sampled-data ODE–PDE systems and application to observer design. *IEEE Transactions on Automatic Control*, *62*(6), 3091–3098.

Albertos, Pedro, & Salt, Julián (2011). Non-uniform sampled-data control of MIMO systems. *Annual Reviews in Control*, *35*, 65–76.

Ames, Aaron D., Coogan, Samuel, Egerstedt, Magnus, Notomista, Gennaro, Sreenath, Koushil, & Tabuada, Paulo (2019). Control barrier functions: Theory and applications. In *2019 18th European Control Conference* (pp. 3420–3431).

Ames, Aaron D., Xu, Xiangru, Grizzle, Jessy W., & Tabuada, Paulo (2017). Control barrier function based quadratic programs for safety critical systems. *IEEE Transactions on Automatic Control*, *62*(8), 3861–3876.

Amin, Saurabh, Litrico, Xavier, Sastry, S. Shankar, & Bayen, Alexandre M. (2013a). Cyber security of water SCADA Systems—Part I: Analysis and experimentation of stealthy deception attacks. *IEEE Transactions on Control Systems Technology*, *21*(5), 1963–1970.

Amin, Saurabh, Litrico, Xavier, Sastry, S. Shankar, & Bayen, Alexandre M. (2013b). Cyber security of water SCADA Systems—Part II: Attack detection using enhanced hydrodynamic models. *IEEE Transactions on Control Systems Technology*, *21*(5), 1679–1693.

Anfinsen, Henrik, & Aamo, Ole Morten (2015). Disturbance rejection in the interior domain of linear 2×2 hyperbolic systems. *IEEE Transactions on Automatic Control*, *60*(1), 186–191.

Anfinsen, Henrik, & Aamo, Ole Morten (2018). Control of a time-variant 1-D linear hyperbolic PDE using infinite-dimensional backstepping. In *2018 26th Mediterranean Conference on Control and Automation* (pp. 108–113).

Anfinsen, Henrik, & Aamo, Ole Morten (2020). Stabilization and tracking control of a time-variant linear hyperbolic PIDE using backstepping. *Automatica*, *116*, Article 108929.

Anta, Adolfo, & Tabuada, Paulo (2010). To sample or not to sample: Self-triggered control for nonlinear systems. *IEEE Transactions on Automatic Control*, *55*(9), 2030–2042.

Årzén, Karl-Erik (1999). A simple event-based PID controller. *IFAC Proceedings Volumes*, *32*(2), 8687–8692, 14th IFAC World Congress 1999, Beijing, China, 5-9 July.

Åström, Karl Johan, & Bernhardsson, Bo (1999). Comparison of periodic and event based sampling for first-order stochastic systems. *IFAC Proceedings Volumes*, *32*(2), 5006–5011, 14th IFAC World Congress 1999, Beijing, China, 5-9 July.

Åström, Karl Johan, & Wittenmark, Björn (1984). *Computer controlled systems : Theory and design* (1st ed.). Prentice-Hall.

Athans, Michael (1972). On the determination of optimal costly measurement strategies for linear stochastic systems. *Automatica*, *8*(4), 397–412.

Auriol, Jean, & Di Meglio, Florent (2020). Robust output feedback stabilization for two heterodirectional linear coupled hyperbolic PDEs. *Automatica*, *115*, Article 108896.

Bagheri, Mostafa, Karafyllis, Iasson, Naseradinmousavi, Peiman, & Krstić, Miroslav (2021). Adaptive control of a two-link robot using batch least-square identifier. *IEEE/CAA Journal of Automatica Sinica*, *8*(1), 86–93.

Bahavarnia, MirSaleh, Tabuada, Paulo, Somarakis, Christoforos, & Motee, Nader (2017). Improving sparsity in time and space via self-triggered sparse optimal controllers. In *2017 IEEE 56th annual Conference on Decision and Control* (pp. 4199–4204).

Balogun, O. S., Hubbard, M., & DeVries, J. J. (1988). Automatic control of canal flow using linear quadratic regulator theory. *Journal of Hydraulic Engineering*, *114*(1), 75–102.

Barré de Saint-Venant, Adhémar-Jean-Claude (1871). Théorie du mouvement non-permanent des eaux, avec application aux crues des rivières et à l'introduction des marées dans leur lit. *Comptes Rendus de L'Académie Des Sciences*, *73*, 147–154, 237–240.

Baudouin, Lucie, Marx, Swann, & Tarbouriech, Sophie (2019). Event-triggered damping of a linear wave equation. *IFAC-PapersOnLine*, *52*(2), 58–63, 3rd IFAC Workshop on Control of Systems Governed by Partial Differential Equations CPDE 2019.

Bemporad, Alberto, Heemels, Maurice, & Johansson, Mikael (2010). *Networked control systems*: *406*, Springer.

Bhan, Luke, Shi, Yuanyuan, & Krstić, Miroslav (2024). Neural operators for bypassing gain and control computations in PDE backstepping. *IEEE Transactions on Automatic Control*, *69*(8), 5310–5325.

Bini, Enrico, & Buttazzo, Giuseppe M. (2014). The optimal sampling pattern for linear control systems. *IEEE Transactions on Automatic Control*, *59*(1), 78–90.

Borgers, D. P., Postoyan, R., Anta, A., Tabuada, P., Nešić, D., & Heemels, W. P. M. H. (2018). Periodic event-triggered control of nonlinear systems using overapproximation techniques. *Automatica*, *94*, 81–87.

Brunner, Florian David, Heemels, W. P. M. H., & Allgöwer, Frank (2019). Event-triggered and self-triggered control for linear systems based on reachable sets. *Automatica*, *101*, 15–26.

Cao, Zhiru, Niu, Yugang, & Zou, Yuanyuan (2023). Self-triggered multi-mode control of Markovian jump systems. *Automatica*, *149*, Article 110837.

Chen, Tongwen, & Francis, Bruce A. (1995). *Optimal sampled-data control systems*. Springer.

Cheng, Meng-Bi, Radisavljevic, Verica, Chang, Chung-Cheng, Lin, Chia-Fu, & Su, Wu-Chung (2009). A sampled-data singularly perturbed boundary control for a heat conduction system with noncollocated observation. *IEEE Transactions on Automatic Control*, *54*(6), 1305–1310.

Conde, Gregory, Quijano, Nicanor, & Ocampo-Martinez, Carlos (2021). Modeling and control in open-channel irrigation systems: A review. *Annual Reviews in Control*, *51*, 153–171.

Coron, Jean-Michel, Hu, Long, Olive, Guillaume, & Shang, Peipei (2021). Boundary stabilization in finite time of one-dimensional linear hyperbolic balance laws with coefficients depending on time and space. *Journal of Differential Equations*, *271*, 1109–1170.

Coron, J. M., d'Andréa Novel, B., & Bastin, G. (1999). A Lyapunov approach to control irrigation canals modeled by Saint-Venant equations. In *1999 European Control Conference* (pp. 3178–3183).

Coutinho, Pedro Henrique Silva, & Palhares, Reinaldo Martínez (2022). Codesign of dynamic event-triggered gain-scheduling control for a class of nonlinear systems. *IEEE Transactions on Automatic Control*, *67*(8), 4186–4193.

Coutinho, Pedro H. S., Peixoto, Márcia L. C., Bessa, Iury, & Palhares, Reinaldo Martinez (2022). Dynamic event-triggered gain-scheduling control of discrete-time quasi-LPV systems. *Automatica*, *141*, Article 110292.

Davó, Miguel Angel, Bresch-Pietri, Delphine, Prieur, Christophe, & Di Meglio, Florent (2019). Stability analysis of a 2×2 linear hyperbolic system with a sampled-data controller via backstepping method and looped-functionals. *IEEE Transactions on Automatic Control*, *64*(4), 1718–1725.

de Halleux, J., Prieur, C., Coron, J.-M., d'Andréa Novel, B., & Bastin, G. (2003). Boundary feedback control in networks of open channels. *Automatica*, *39*(8), 1365–1376.

Demir, Cenk, Diagne, Mamadou, & Krstić, Miroslav (2024a). Periodic event-triggered boundary control of neuron growth with actuation at soma. In *2024 IEEE 63rd Conference on Decision and Control* (pp. 434–439).

Demir, Cenk, Koga, Shumon, & Krstić, Miroslav (2024b). Event-triggered control of neuron growth with actuation at soma. In *2024 American Control Conference* (pp. 5301–5306).

Demirel, Burak, Leong, Alex S., Gupta, Vijay, & Quevedo, Daniel E. (2019). Tradeoffs in stochastic event-triggered control. *IEEE Transactions on Automatic Control*, *64*(6), 2567–2574.

Deutschmann, Andreas, Jadachowski, Lukas, & Kugi, Andreas (2016). Backstepping-based boundary observer for a class of time-varying linear hyperbolic PIDEs. *Automatica*, *68*, 369–377.

Di Meglio, Florent, Vazquez, Rafael, & Krstić, Miroslav (2013). Stabilization of a system of $n+1$ coupled first-order hyperbolic linear PDEs with a single boundary input. *IEEE Transactions on Automatic Control*, *58*(12), 3097–3111.

Diagne, Ababacar, Bastin, Georges, & Coron, Jean-Michel (2012). Lyapunov exponential stability of 1-D linear hyperbolic systems of balance laws. *Automatica*, *48*(1), 109–114.

Diagne, Ababacar, Diagne, Mamadou, Tang, Shuxia, & Krstić, Miroslav (2017). Backstepping stabilization of the linearized Saint-Venant–Exner model. *Automatica*, *76*, 345–354.

Diagne, Mamadou, & Karafyllis, Iasson (2021). Event-triggered boundary control of a continuum model of highly re-entrant manufacturing systems. *Automatica*, *134*, Article 109902.

Diagne, Mamadou, Tang, Shu-Xia, Diagne, Ababacar, & Krstić, Miroslav (2017). Control of shallow waves of two unmixed fluids by backstepping. *Annual Reviews in Control*, *44*, 211–225.

Dolk, V. S., Borgers, D. P., & Heemels, W. P. M. H. (2014). Dynamic event-triggered control: Tradeoffs between transmission intervals and performance. In *53rd IEEE Conference on Decision and Control* (pp. 2764–2769).

Dolk, Victor, & Heemels, Maurice (2017). Event-triggered control systems under packet losses. *Automatica*, *80*, 143–155.

Donkers, M. C. F., & Heemels, W. P. M. H. (2012). Output-based event-triggered control with guaranteed L_∞-gain and improved and decentralized event-triggering. *IEEE Transactions on Automatic Control*, *57*(6), 1362–1376.

Dorf, R., Farren, M., & Phillips, C. (1962). Adaptive sampling frequency for sampled-data control systems. *IRE Transactions on Automatic Control*, *7*(1), 38–47.

Eliades, Demetrios G., Vrachimis, Stelios G., Moghaddam, Alireza, Tzortzis, Ioannis, & Polycarpou, Marios M. (2023). Contamination event diagnosis in drinking water networks: A review. *Annual Reviews in Control*, *55*, 420–441.

Espitia, Nicolás (2020). Observer-based event-triggered boundary control of a linear 2×2 hyperbolic systems. *Systems & Control Letters*, *138*, Article 104668.

Espitia, Nicolás, & Auriol, Jean (2025). Event-triggered gain scheduling of 2×2 linear hyperbolic PDEs with time and space varying coupling coefficients. *Automatica*, *179*, Article 112455.

Espitia, Nicolás, Auriol, Jean, Yu, Huan, & Krstić, Miroslav (2022a). Event-triggered output feedback control of traffic flow on cascaded roads. In *Advances in distributed parameter systems* (pp. 243–267). Springer.

Espitia, Nicolás, Auriol, Jean, Yu, Huan, & Krstić, Miroslav (2022b). Traffic flow control on cascaded roads by event-triggered output feedback. *International Journal of Robust and Nonlinear Control*, *32*(10), 5919–5949.

Espitia, Nicolás, Girard, Antoine, Marchand, Nicolas, & Prieur, Christophe (2016). Event-based control of linear hyperbolic systems of conservation laws. *Automatica*, *70*, 275–287.

Espitia, Nicolás, Girard, Antoine, Marchand, Nicolas, & Prieur, Christophe (2018). Event-based boundary control of a linear 2×2 hyperbolic system via backstepping approach. *IEEE Transactions on Automatic Control*, *63*(8), 2686–2693.

Espitia, Nicolás, Karafyllis, Iasson, & Krstić, Miroslav (2021). Event-triggered boundary control of constant-parameter reaction–diffusion PDEs: A small-gain approach. *Automatica*, *128*, Article 109562.

Espitia, Nicolás, Yu, Huan, & Krstić, Miroslav (2020). Event-triggered varying speed limit control of stop-and-go traffic. *IFAC-PapersOnLine*, *53*(2), 7509–7514, 21st IFAC World Congress.

Etienne, Lucien, Langueh, Kokou, & Rajaoarisoa, Lala (2022). Self triggered controller co-design using LASSO regression. In *2022 30th Mediterranean Conference on Control and Automation* (pp. 139–144).

Fridman, Emilia, & Bar Am, Netzer (2013). Sampled-data distributed H_∞ control of transport reaction systems. *SIAM Journal on Control and Optimization*, *51*(2), 1500–1527.

Fu, Anqi, & Mazo, Manuel (2018). Decentralized periodic event-triggered control with quantization and asynchronous communication. *Automatica*, *94*, 294–299.

Gao, Yong-Feng, Sun, Xi-Ming, Wen, Changyun, & Wang, Wei (2018). Event-triggered control for stochastic nonlinear systems. *Automatica*, *95*, 534–538.

Ge, Xiaohua, Han, Qing-Long, Zhang, Xian-Ming, & Ding, Derui (2021). Dynamic event-triggered control and estimation: A survey. *Machine Intelligence Research*, *18*(6), 857–886.

Ghodrat, Mohsen, & Marquez, Horacio J. (2023). A new Lyapunov-based event-triggered control of linear systems. *IEEE Transactions on Automatic Control*, *68*(4), 2599–2606.

Girard, Antoine (2015). Dynamic triggering mechanisms for event-triggered control. *IEEE Transactions on Automatic Control*, *60*(7), 1992–1997.

Gleizer, Gabriel de Albuquerque, & Mazo, Manuel (2020). Self-triggered output-feedback control of LTI systems subject to disturbances and noise. *Automatica*, *120*, Article 109129.

Gupta, S. (1963). Increasing the sampling efficiency for a control system. *IEEE Transactions on Automatic Control*, *8*(3), 263–264.

Hashimoto, Kazumune, Onoue, Yuga, Ogura, Masaki, & Ushio, Toshimitsu (2021). Event-triggered control for mitigating SIS spreading processes. *Annual Reviews in Control*, *52*, 479–494.

Heemels, W. P. M. H., & Donkers, M. C. F. (2013). Model-based periodic event-triggered control for linear systems. *Automatica*, *49*(3), 698–711.

Heemels, W. P. M. H., Donkers, M. C. F., & Teel, Andrew R. (2013). Periodic event-triggered control for linear systems. *IEEE Transactions on Automatic Control*, *58*(4), 847–861.

Heemels, W. P. M. H., Johansson, K. H., & Tabuada, P. (2012). An introduction to event-triggered and self-triggered control. In *2012 51st IEEE Conference on Decision and Control* (pp. 3270–3285).

Hertneck, Michael, Meister, David, & Allgöwer, Frank (2026). Current trends and future directions in event-based control. *European Journal of Control*, *87*, Article 101387.

Hespanha, João P., Liberzon, Daniel, & Morse, A. Stephen (2003). Overcoming the limitations of adaptive control by means of logic-based switching. *Systems & Control Letters*, *49*(1), 49–65.

Hespanha, João P., Naghshtabrizi, Payam, & Xu, Yonggang (2007). A survey of recent results in networked control systems. *Proceedings of the IEEE*, *95*(1), 138–162.

Hu, Long, Di Meglio, Florent, Vazquez, Rafael, & Krstić, Miroslav (2016). Control of homodirectional and general heterodirectional linear coupled hyperbolic PDEs. *IEEE Transactions on Automatic Control*, *61*(11), 3301–3314.

Imer, O. C., & Basar, T. (2005). Optimal estimation with limited measurements. In *Proceedings of the 44th IEEE Conference on Decision and Control* (pp. 1029–1034).

Imer, O. C., & Basar, T. (2006). Optimal control with limited controls. In *2006 American Control Conference* (pp. 298–303).

Jury, Eliahu I. (1956). Synthesis and critical study of sampled-data control systems. *Transactions of the American Institute of Electrical Engineers, Part II: Applications and Industry*, *75*(3), 141–151.

Kalman, R. E., & Bertram, J. E. (1959). A unified approach to the theory of sampling systems. *Journal of the Franklin Institute*, *267*(5), 405–436.

Kang, Wen, & Fridman, Emilia (2022). Sampled-data control of 2-D Kuramoto–Sivashinsky equation. *IEEE Transactions on Automatic Control*, *67*(3), 1314–1326.

Kang, Wen, Fridman, Emilia, Zhang, Jing, & Liu, Chuan-Xin (2023). Event-triggered stabilization of parabolic PDEs by switching. In *2023 62nd IEEE Conference on Decision and Control* (pp. 6899–6904).

Karafyllis, Iasson, Espitia, Nicolás, & Krstić, Miroslav (2021). Event-triggered gain scheduling of reaction-diffusion PDEs. *SIAM Journal on Control and Optimization*, *59*(3), 2047–2067.

Karafyllis, Iasson, Kontorinaki, Maria, & Krstić, Miroslav (2020). Adaptive control by regulation-triggered batch least squares. *IEEE Transactions on Automatic Control*, *65*(7), 2842–2855.

Karafyllis, Iasson, & Krstić, Miroslav (2012). Nonlinear stabilization under sampled and delayed measurements, and with inputs subject to delay and zero-order hold. *IEEE Transactions on Automatic Control*, *57*(5), 1141–1154.

Karafyllis, I., & Krstić, M. (2016). Approximate and sampled-data predictors for control of nonlinear delay systems. *Annual Reviews in Control*, *41*, 2–12.

Karafyllis, Iasson, & Krstić, Miroslav (2017). Stability of integral delay equations and stabilization of age-structured models. *ESAIM. Control, Optimisation and Calculus of Variations*, *23*(4), 1667–1714.

Karafyllis, Iasson, & Krstić, Miroslav (2018). Sampled-data boundary feedback control of 1-D parabolic PDEs. *Automatica*, *87*, 226–237.

Karafyllis, Iasson, & Krstić, Miroslav (2025). *Robust adaptive control: Deadzone-adapted disturbance suppression*. SIAM.

Katz, Rami, Fridman, Emilia, & Selivanov, Anton (2021). Boundary delayed observer-controller design for reaction–diffusion systems. *IEEE Transactions on Automatic Control*, *66*(1), 275–282.

Koga, Shumon, Demir, Cenk, & Krstić, Miroslav (2023). Event-triggered safe stabilizing boundary control for the Stefan PDE system with actuator dynamics. In *2023 American Control Conference* (pp. 1794–1799).

Koga, Shumon, Karafyllis, Iasson, & Krstić, Miroslav (2021). Towards implementation of PDE control for Stefan system: Input-to-state stability and sampled-data design. *Automatica*, *127*, Article 109538.

Koudohode, Florent, Baudouin, Lucie, & Tarbouriech, Sophie (2022). Event-based control of a damped linear wave equation. *Automatica*, *146*, Article 110627.

Koudohode, Florent, Espitia, Nicolás, & Krstić, Miroslav (2024). Event-triggered boundary control of an unstable reaction diffusion PDE with input delay. *Systems & Control Letters*, *186*, Article 105775.

Krstić, Miroslav (2024). Inverse optimal safety filters. *IEEE Transactions on Automatic Control*, *69*(1), 16–31.

Krstić, Miroslav, & Bekiaris-Liberis, Nikolaos (2013). Nonlinear stabilization in infinite dimension. *Annual Reviews in Control*, *37*(2), 220–231.

Krstić, Miroslav, & Smyshlyaev, Andrey (2008). Adaptive control of PDEs. *Annual Reviews in Control*, *32*(2), 149–160.

Lamarque, Maxence, Bhan, Luke, Shi, Yuanyuan, & Krstić, Miroslav (2025). Adaptive neural-operator backstepping control of a benchmark hyperbolic PDE. *Automatica*, *177*, Article 112329.

Leong, Alex S., Quevedo, Daniel E., & Dey, Subhrakanti (2017). Optimal transmission scheduling for event-triggered estimation with packet drops. In *Optimal control of energy resources for state estimation over wireless channels* (pp. 35–64). Springer.

Lhachemi, Hugo (2024). Event-triggered finite-dimensional observer-based output feedback stabilization of reaction–diffusion PDEs. *IEEE Transactions on Automatic Control*, *69*(8), 5651–5657.

Linsenmayer, Steffen, Dimarogonas, Dimos V., & Allgöwer, Frank (2019). Periodic event-triggered control for networked control systems based on non-monotonic Lyapunov functions. *Automatica*, *106*, 35–46.

Linvill, William K. (1951). Sampled-data control systems studied through comparison of sampling with amplitude modulation. *Transactions of the American Institute of Electrical Engineers*, *70*(2), 1779–1788.

Litrico, Xavier, & Fromion, Vincent (2009). *Modeling and control of hydrosystems*. Springer Science & Business Media.

Luo, Shixian, & Deng, Feiqi (2020). On event-triggered control of nonlinear stochastic systems. *IEEE Transactions on Automatic Control*, *65*(1), 369–375.

Marchand, Nicolas, Durand, Sylvain, & Guerrero Castellanos, Jose Fermi (2013). A general formula for event-based stabilization of nonlinear systems. *IEEE Transactions on Automatic Control*, *58*(5), 1332–1337.

Martins, Valérie Dos Santos, Rodrigues, Mickael, & Diagne, Mamadou (2012). A multi-model approach to Saint-Venant equations: A stability study by LMIs. *International Journal of Applied Mathematics and Computer Science*, *22*(3), 539–550.

Mazo, Manuel, Anta, Adolfo, & Tabuada, Paulo (2009). On self-triggered control for linear systems: Guarantees and complexity. In *2009 European Control Conference* (pp. 3767–3772).

Mazo, Manuel, Anta, Adolfo, & Tabuada, Paulo (2010). An ISS self-triggered implementation of linear controllers. *Automatica*, *46*(8), 1310–1314.

Mazo, Manuel, & Tabuada, Paulo (2008). On event-triggered and self-triggered control over sensor/actuator networks. In *2008 47th IEEE Conference on Decision and Control* (pp. 435–440).

Meier, L., Peschon, J., & Dressler, R. (1967). Optimal control of measurement subsystems. *IEEE Transactions on Automatic Control*, *12*(5), 528–536.

Miller, D. E., & Davison, E. J. (1988). An adaptive controller which provides Lyapunov stability. In *Proceedings of the 27th IEEE Conference on Decision and Control*: *3*, (pp. 1934–1940).

Miller, D. E., & Davison, E. J. (1991). An adaptive controller which provides an arbitrarily good transient and steady-state response. *IEEE Transactions on Automatic Control*, *36*(1), 68–81.

Morse, A. S. (1996). Supervisory control of families of linear set-point controllers - Part I. Exact matching. *IEEE Transactions on Automatic Control*, *41*(10), 1413–1431.

Nasir, Hasan A., Cantoni, Michael, Li, Yuping, & Weyer, Erik (2021). Stochastic model predictive control based reference planning for automated open-water channels. *IEEE Transactions on Control Systems Technology*, *29*(2), 607–619.

Nešić, Dragan, & Laila, Dina Shona (2002). A note on input-to-state stabilization for nonlinear sampled-data systems. *IEEE Transactions on Automatic Control*, *47*(7), 1153–1158.

Nešić, Dragan, & Teel, Andrew R. (2004). A framework for stabilization of nonlinear sampled-data systems based on their approximate discrete-time models. *IEEE Transactions on Automatic Control*, *49*(7), 1103–1122.

Nešić, D., Teel, A. R., & Kokotović, P. V. (1999). Sufficient conditions for stabilization of sampled-data nonlinear systems via discrete-time approximations. *Systems & Control Letters*, *38*(4–5), 259–270.

Nešić, D., Teel, A. R., & Sontag, E. D. (1999). Formulas relating KL stability estimates of discrete-time and sampled-data nonlinear systems. *Systems & Control Letters*, *38*(1), 49–60.

Nozari, Erfan, Tallapragada, Pavankumar, & Cortés, Jorge (2020). Event-triggered stabilization of nonlinear systems with time-varying sensing and actuation delay. *Automatica*, *113*, Article 108754.

Nyquist, H. (1928). Certain topics in telegraph transmission theory. *Transactions of the American Institute of Electrical Engineers*, *47*(2), 617–644.

Ong, Pio, & Cortés, Jorge (2024). Performance-barrier-based event-triggered control with applications to network systems. *IEEE Transactions on Automatic Control*, *69*(7), 4230–4244.

Pessim, Paulo Sergio Pereira, Coutinho, Pedro Henrique Silva, Lacerda, Márcio J., Puig, Vicenç, & Palhares, Reinaldo Martinez (2025). A distributed gain-scheduled observer-based approach for the practical consensus of LPV multi-agent systems. *Automatica*, *177*, Article 112353.

Postoyan, Romain, Tabuada, Paulo, Nešić, Dragan, & Anta, Adolfo (2015). A framework for the event-triggered stabilization of nonlinear systems. *IEEE Transactions on Automatic Control*, *60*(4), 982–996.

Prieur, Christophe, Girard, Antoine, & Witrant, Emmanuel (2014). Stability of switched linear hyperbolic systems by Lyapunov techniques. *IEEE Transactions on Automatic Control*, *59*(8), 2196–2202.

Prieur, Christophe, & Mazenc, Frédéric (2012). ISS-Lyapunov functions for time-varying hyperbolic systems of balance laws. *Mathematics of Control, Signals, and Systems*, *24*(1), 111–134.

Prieur, Christophe, & Winkin, Joseph J. (2018). Boundary feedback control of linear hyperbolic systems: Application to the Saint-Venant–Exner equations. *Automatica*, *89*, 44–51.

Qi, Jie, Vazquez, Rafael, & Krstić, Miroslav (2015). Multi-agent deployment in 3-D via PDE control. *IEEE Transactions on Automatic Control*, *60*(4), 891–906.

Qi, Jie, Wang, Shanshan, Fang, Jian-an, & Diagne, Mamadou (2019). Control of multi-agent systems with input delay via PDE-based method. *Automatica*, *106*, 91–100.

Ragazzini, J. R., & Zadeh, L. A. (1952). The analysis of sampled-data systems. *Transactions of the American Institute of Electrical Engineers, Part II: Applications and Industry*, *71*(5), 225–234.

Rathnayake, Bhathiya, & Diagne, Mamadou (2022). Event-based boundary control of one-phase Stefan problem: A static triggering approach. In *2022 American Control Conference* (pp. 2403–2408).

Rathnayake, Bhathiya, & Diagne, Mamadou (2023). Observer-based periodic event-triggered boundary control of the one-phase Stefan problem. *IFAC-PapersOnLine*, *56*(2), 11415–11422, 22nd IFAC World Congress.

Rathnayake, Bhathiya, & Diagne, Mamadou (2024a). Observer-based event-triggered boundary control of the one-phase Stefan problem. *International Journal of Control*, *97*(12), 2975–2986.

Rathnayake, Bhathiya, & Diagne, Mamadou (2024b). Observer-based periodic event-triggered and self-triggered boundary control of a class of parabolic PDEs. *IEEE Transactions on Automatic Control*, *69*(12), 8836–8843.

Rathnayake, Bhathiya, & Diagne, Mamadou (2025). Sampled-data boundary control of a class of reaction-diffusion PDEs: A Lyapunov-based approach. In *2025 American Control Conference* (pp. 2426–2431).

Rathnayake, Bhathiya, & Diagne, Mamadou (2026). Global exponential stabilization of 2×2 linear hyperbolic PDEs via dynamic event-triggered backstepping control. *Automatica*, *183*, Article 112617.

Rathnayake, Bhathiya, Diagne, Mamadou, Cortés, Jorge, & Krstić, Miroslav (2024). Performance-barrier-based event-triggered boundary control of a class of reaction-diffusion PDEs. In *2024 American Control Conference* (pp. 5313–5319).

Rathnayake, Bhathiya, Diagne, Mamadou, Cortés, Jorge, & Krstić, Miroslav (2025). Performance-barrier event-triggered control of a class of reaction–diffusion PDEs. *Automatica*, *174*, Article 112181.

Rathnayake, Bhathiya, Diagne, Mamadou, Espitia, Nicolás, & Karafyllis, Iasson (2022). Observer-based event-triggered boundary control of a class of reaction–diffusion PDEs. *IEEE Transactions on Automatic Control*, *67*(6), 2905–2917.

Rathnayake, Bhathiya, Diagne, Mamadou, & Karafyllis, Iasson (2022). Sampled-data and event-triggered boundary control of a class of reaction–diffusion PDEs with collocated sensing and actuation. *Automatica*, *137*, Article 110026.

Seidel, Marc, Hertneck, Michael, Yu, Pian, Linsenmayer, Steffen, Dimarogonas, Dimos V., & Allgöwer, Frank (2024). A window-based periodic event-triggered consensus scheme for multiagent systems. *IEEE Transactions on Control of Network Systems*, *11*(1), 414–426.

Selivanov, Anton, & Fridman, Emilia (2016). Distributed event-triggered control of diffusion semilinear PDEs. *Automatica*, *68*, 344–351.

Selivanov, Anton, & Fridman, Emilia (2017). Sampled-data relay control of diffusion PDEs. *Automatica*, *82*, 59–68.

Seuret, Alexandre, & Prieur, Christophe (2011). Event-triggered sampling algorithms based on a Lyapunov function. In *2011 50th IEEE Conference on Decision and Control and European Control Conference* (pp. 6128–6133).

Shannon, C. E. (1949). Communication in the presence of noise. *Proceedings of the IRE*, *37*(1), 10–21.

Simonovic, Slobodan P., & Akter, Taslima (2006). Participatory floodplain management in the Red River Basin, Canada. *Annual Reviews in Control*, *30*(2), 183–192.

Smyshlyaev, Andrey, & Krstić, Miroslav (2010). *Adaptive control of parabolic PDEs*. Princeton University Press.

Somathilake, Eranda, & Diagne, Mamadou (2024). Output feedback control of suspended sediment load entrainment in water canals and reservoirs. *IFAC-PapersOnLine*, *58*(28), 983–988, The 4th Modeling, Estimation, and Control Conference – 2024.

Somathilake, Eranda, Rathnayake, Bhathiya, & Diagne, Mamadou (2025). Output feedback periodic event-triggered and self-triggered boundary control of coupled 2×2 linear hyperbolic PDEs. *Automatica*, *179*, Article 112433.

Strecker, Timm, Cantoni, Michael, & Aamo, Ole Morten (2024). Event-triggered boundary control of semilinear hyperbolic systems. *IEEE Transactions on Automatic Control*, *69*(1), 418–425.

Sun, Libei, Song, Yongduan, Lv, Maolong, Huang, Xiucai, & Wen, Changyun (2025). Event-triggered adaptive safe-oriented barrier Lyapunov function-based boundary control of flexible beam systems characterized by uncertain Euler–Bernoulli PDEs. *Automatica*, *182*, Article 112555.

Swamee, Prabhata K. (1992). Sluice-gate discharge equations. *Journal of Irrigation and Drainage Engineering*, *118*(1), 56–60.

Szymanek, Aleksandra, Gleizer, Gabriel de Albuquerque., & Mazo, Manuel (2019). Periodic event-triggered control with a relaxed triggering condition. In *2019 IEEE 58th Conference on Decision and Control* (pp. 1656–1661).

Tabuada, Paulo (2007). Event-triggered real-time scheduling of stabilizing control tasks. *IEEE Transactions on Automatic Control*, *52*(9), 1680–1685.

Tallapragada, Pavankumar, & Chopra, Nikhil (2013). On event triggered tracking for nonlinear systems. *IEEE Transactions on Automatic Control*, *58*(9), 2343–2348.

Taylor, Andrew J., Ong, Pio, Cortés, Jorge, & Ames, Aaron D. (2021). Safety-critical event triggered control via input-to-state safe barrier functions. *IEEE Control Systems Letters*, *5*(3), 749–754.

Tomovic, R., & Bekey, G. (1966). Adaptive sampling based on amplitude sensitivity. *IEEE Transactions on Automatic Control*, *11*(2), 282–284.

Tripathy, Niladri Sekhar, Kar, I. N., & Paul, Kolin (2017). Stabilization of uncertain discrete-time linear system with limited communication. *IEEE Transactions on Automatic Control*, *62*(9), 4727–4733.

Vazquez, Rafael, & Krstić, Miroslav (2017). Boundary control of coupled reaction-advection-diffusion systems with spatially-varying coefficients. *IEEE Transactions on Automatic Control*, *62*(4), 2026–2033.

Vazquez, Rafael, Krstić, Miroslav, & Coron, Jean-Michel (2011). Backstepping boundary stabilization and state estimation of a 2×2 linear hyperbolic system. In *2011 50th IEEE Conference on Decision and Control and European Control Conference* (pp. 4937–4942).

Wahlin, Brian, & Zimbelman, Darell (2018). Canal automation for irrigation systems: American Society of Civil Engineers manual of practice number 131. *Irrigation and Drainage*, *67*(1), 22–28.

Wakaiki, Masashi, & Sano, Hideki (2020). Event-triggered control of infinite-dimensional systems. *SIAM Journal on Control and Optimization*, *58*(2), 605–635.

Wakaiki, Masashi, & Sano, Hideki (2022). Stability analysis of infinite-dimensional event-triggered and self-triggered control systems with Lipschitz perturbations. *Mathematical Control and Related Fields*, *12*(1), 245–273.

Wan, Haiying, Luan, Xiaoli, Karimi, Hamid Reza, & Liu, Fei (2021). Dynamic self-triggered controller codesign for Markov jump systems. *IEEE Transactions on Automatic Control*, *66*(3), 1353–1360.

Wang, Ji, & Diagne, Mamadou (2024). Delay-adaptive boundary control of coupled hyperbolic PDE-ODE cascade systems. *IEEE Transactions on Automatic Control*, *69*(12), 8156–8171.

Wang, Shanshan, Diagne, Mamadou, & Krstić, Miroslav (2025a). Backstepping neural operators for $2\times$ 2 hyperbolic PDEs. *Automatica*, *178*, Article 112351.

Wang, Shanshan, Diagne, Mamadou, & Krstić, Miroslav (2025b). Deep learning of delay-compensated backstepping for reaction–diffusion PDEs. *IEEE Transactions on Automatic Control*, *70*(6), 4209–4216.

Wang, Shanshan, Diagne, Mamadou, & Qi, Jie (2024). Delay-adaptive compensation for 3-D formation control of leader-actuated multi-agent systems. *Automatica*, *164*, Article 111645.

Wang, Pengfei, & Fridman, Emilia (2024). Sampled-data finite-dimensional observer-based control of 1D stochastic parabolic PDEs. *SIAM Journal on Control and Optimization*, *62*(1), 297–325.

Wang, Ji, & Krstić, Miroslav (2021). Adaptive event-triggered PDE control for load-moving cable systems. *Automatica*, *129*, Article 109637.

Wang, Ji, & Krstić, Miroslav (2022a). *PDE control of string-actuated motion*: *76*, Princeton University Press.

Wang, Ji, & Krstić, Miroslav (2022b). Delay-compensated event-triggered boundary control of hyperbolic PDEs for deep-sea construction. *Automatica*, *138*, Article 110137.

Wang, Ji, & Krstić, Miroslav (2022c). Event-triggered output-feedback backstepping control of sandwich hyperbolic PDE systems. *IEEE Transactions on Automatic Control*, *67*(1), 220–235.

Wang, Ji, & Krstić, Miroslav (2023a). Event-triggered adaptive control of a parabolic PDE–ODE cascade with piecewise-constant inputs and identification. *IEEE Transactions on Automatic Control*, *68*(9), 5493–5508.

Wang, Ji, & Krstić, Miroslav (2023b). Event-triggered adaptive control of coupled hyperbolic PDEs with piecewise-constant inputs and identification. *IEEE Transactions on Automatic Control*, *68*(3), 1568–1583.

Wang, Ji, Krstić, Miroslav, & Karafyllis, Iasson (2021). Adaptive regulation- triggered control of hyperbolic PDEs by batch least-squares. In *2021 American Control Conference* (pp. 4057–4062).

Wang, Xiaofeng, & Lemmon, Michael D. (2008). Event design in event-triggered feedback control systems. In *2008 47th IEEE Conference on Decision and Control* (pp. 2105–2110).

Wang, Wei, Postoyan, Romain, Nešić, Dragan, & Heemels, W. P. M. H. (2020). Periodic event-triggered control for nonlinear networked control systems. *IEEE Transactions on Automatic Control*, *65*(2), 620–635.

Wang, Tong, Wang, Nan, Qiu, Jianbin, Buccella, Concettina, & Cecati, Carlo (2023). Adaptive event-triggered control of stochastic nonlinear systems with unknown dead zone. *IEEE Transactions on Fuzzy Systems*, *31*(1), 138–147.

Wang, Yingchun, Zheng, Wei Xing, & Zhang, Huaguang (2017). Dynamic event-based control of nonlinear stochastic systems. *IEEE Transactions on Automatic Control*, *62*(12), 6544–6551.

Widrow, B. (1960). Adaptive sampled-data systems. In *Proceedings of the First International Congress of the International Federation of Automatic Control* (pp. 406–411).

Yamamoto, Yutaka (2019). The influence of R. E. Kalman—state space theory, realization, and sampled-data systems. *Annual Reviews in Control*, *47*, 1–6.

Yang, Guang, Belta, Calin, & Tron, Roberto (2019). Self-triggered control for safety critical systems using control barrier functions. In *2019 American Control Conference* (pp. 4454–4459).

Yi, Xinlei, Liu, Kun, Dimarogonas, Dimos V., & Johansson, Karl H. (2019). Dynamic event-triggered and self-triggered control for multi-agent systems. *IEEE Transactions on Automatic Control*, *64*(8), 3300–3307.

Yuan, Hongpeng, Wang, Ji, & Diagne, Mamadou (2025). DeepONet of dynamic event-triggered backstepping boundary control for reaction-diffusion PDEs. In *2025 IEEE 64th Conference on Decision and Control* (pp. 2989–2994).

Zhang, Jin, & Fridman, Emilia (2021). Dynamic event-triggered control of networked stochastic systems with scheduling protocols. *IEEE Transactions on Automatic Control*, *66*(12), 6139–6147.

Zhang, Xian-Ming, Han, Qing-Long, Ge, Xiaohua, Ning, Boda, & Zhang, Bao-Lin (2023). Sampled-data control systems with non-uniform sampling: A survey of methods and trends. *Annual Reviews in Control*, *55*, 70–91.

Zhang, Pengpeng, Liu, Tengfei, & Jiang, Zhong-Ping (2021a). Event-triggered stabilization of a class of nonlinear time-delay systems. *IEEE Transactions on Automatic Control*, *66*(1), 421–428.

Zhang, Pengpeng, Liu, Tengfei, & Jiang, Zhong-Ping (2021b). Systematic design of robust event-triggered state and output feedback controllers for uncertain nonholonomic systems. *IEEE Transactions on Automatic Control*, *66*(1), 213–228.

Zhang, Peihan, Rathnayake, Bhathiya, Diagne, Mamadou, & Krstić, Miroslav (2025). Performance-barrier event-triggered PDE control of traffic flow. *IEEE Transactions on Automatic Control*, *70*(9), 5720–5735.

Zhang, Kai, Zhou, Bin, Zheng, Wei Xing, & Duan, Guang-Ren (2022). Event-triggered and self-triggered gain scheduled control of linear systems with input constraints. *IEEE Transactions on Systems, Man, and Cybernetics: Systems*, *52*(10), 6452–6463.

Zhao, Yan, & Vazquez, Rafael (2026). Event-triggered boundary estimation for 2×2 hyperbolic PDEs with disturbance. *Automatica*, *183*, Article 112615.